JOURNAL OF PETROLOGY | VOLUME 45 | NUMBER 12 | PAGES 2423–2458 | 2004 | doi:10.1093/petrology/egh068

Bulk-rock Major and Trace Element Compositions of Abyssal Peridotites: Implications for Mantle Melting, Melt Extraction and Post-melting Processes Beneath Mid-Ocean Ridges

YAOLING NIU[1,2]*

[1]DEPARTMENT OF GEOSCIENCES, UNIVERSITY OF HOUSTON, 4800 CALHOUN ROAD, HOUSTON, TX 77204-5007, USA
[2]DEPARTMENT OF EARTH SCIENCES, UNIVERSITY OF DURHAM, DURHAM DH1 3LE, UK

RECEIVED MARCH 22, 2004; ACCEPTED AUGUST 4, 2004
ADVANCE ACCESS PUBLICATION SEPTEMBER 24, 2004

This paper presents the first comprehensive major and trace element data for ~130 abyssal peridotite samples from the Pacific and Indian ocean ridge–transform systems. The data reveal important features about the petrogenesis of these rocks, mantle melting and melt extraction processes beneath ocean ridges, and elemental behaviours. Although abyssal peridotites are serpentinized, and have also experienced seafloor weathering, magmatic signatures remain well preserved in the bulk-rock compositions. The better inverse correlation of MgO with progressively heavier rare earth elements (REE) reflects varying amounts of melt depletion. This melt depletion may result from recent sub-ridge mantle melting, but could also be inherited from previous melt extraction events from the fertile mantle source. Light REE (LREE) in bulk-rock samples are more enriched, not more depleted, than in the constituent clinopyroxenes (cpx) of the same sample suites. If the cpx LREE record sub-ridge mantle melting processes, then the bulk-rock LREE must reflect post-melting refertilization. The significant correlations of LREE (e.g. La, Ce, Pr, Nd) with immobile high field strength elements (HFSE, e.g. Nb and Zr) suggest that enrichments of both LREE and HFSE resulted from a common magmatic process. The refertilization takes place in the 'cold' thermal boundary layer (TBL) beneath ridges through which the ascending melts migrate and interact with the advanced residues. The refertilization apparently did not affect the cpx relics analyzed for trace elements. This observation suggests grain-boundary porous melt migration in the TBL. The ascending melts may not be thermally 'reactive', and thus may have affected only cpx rims, which, together with precipitated olivine, entrapped melt, and the rest of the rock, were subsequently serpentinized. Very large variations in bulk-rock Zr/Hf and Nb/Ta ratios are observed, which are unexpected. The correlation between the two ratios is consistent with observations on basalts that $D_{Zr}/D_{Hf} < 1$ and $D_{Nb}/D_{Ta} < 1$. Given the identical charges (5^+ for Nb and Ta; 4^+ for Zr and Hf) and essentially the same ionic radii ($R_{Nb}/R_{Ta} = 1{\cdot}000$ and $R_{Zr}/R_{Hf} = 1{\cdot}006$–$1{\cdot}026$), yet a factor of ~2 mass differences ($M_{Zr}/M_{Hf} = 0{\cdot}511$ and $M_{Nb}/M_{Ta} = 0{\cdot}513$), it is hypothesized that mass-dependent D values, or diffusion or mass-transfer rates may be important in causing elemental fractionations during porous melt migration in the TBL. It is also possible that some 'exotic' phases with highly fractionated Zr/Hf and Nb/Ta ratios may exist in these rocks, thus having 'nugget' effects on the bulk-rock analyses. All these hypotheses need testing by constraining the storage and distribution of all the incompatible trace elements in mantle peridotite. As serpentine contains up to 13 wt % H_2O, and is stable up to 7 GPa before it is transformed to dense hydrous magnesium silicate phases that are stable at pressures of ~5–50 GPa, it is possible that the serpentinized peridotites may survive, at least partly, subduction-zone dehydration, and transport large amounts of H_2O (also Ba, Rb, Cs, K, U, Sr, Pb, etc. with elevated U/Pb ratios) into the deep mantle. The latter may contribute to the HIMU component in the source regions of some oceanic basalts.

KEY WORDS: *abyssal peridotites; serpentinization; seafloor weathering; bulk-rock major and trace element compositions; mantle melting; melt extraction; melt–residue interaction; porous flows; Nb/Ta and Zr/Hf fractionations; HIMU mantle sources*

*Corresponding author. Telephone: 44-19-1334-2311. Fax: 44-19-1334-2301. Present e-mail: niny@ev1.net. After 1 December 2004: y.niu@durham.ac.uk

INTRODUCTION

The global mid-ocean ridge system is the dynamic expression of the mantle circulation system that governs plate tectonics. Ocean ridge magmatism, which creates the oceanic crust, has received much attention by the Earth Science community since the advent of plate tectonics theory over 30 years ago. It is now widely accepted that plate separation at ocean ridges causes the mantle beneath to rise and to partially melt by decompression. Abyssal peridotites and igneous ocean crust are the two complementary products of such decompression melting. Igneous crust [mid-ocean ridge basalts (MORB) plus dikes and lower-crustal gabbros] represents solidified partial melts whereas abyssal peridotites are melting residues tectonically exposed along fracture zones, within transforms, and locally on rift valley floors at some slow-spreading ridges.

Studies of the two melting products have led to our current notion that mantle potential temperature variation (e.g. Dick & Fisher, 1984; Dick *et al.*, 1984; Michael & Bonatti, 1985; Klein & Langmuir, 1987; McKenzie & Bickle, 1988; Dick, 1989; Johnson *et al.*, 1990; Niu & Batiza, 1991; Langmuir *et al.*, 1992; Niu *et al.*, 1997), plate spreading rate variation (Niu, 1997; Niu & Hékinian, 1997*a*) and mantle source compositional variation (e.g. Natland, 1989; Michael *et al.*, 1994; Shen & Forsyth, 1995; Niu *et al.*, 1996, 2001, 2002*a*) are the three fundamental variables that determine the extent of mantle melting, MORB composition and ocean crust production (Niu *et al.*, 2001). Nevertheless, details of mantle melting (e.g. Langmuir *et al.*, 1992; Kelemen *et al.*, 1997; Niu, 1997, 1999; Asimow, 1999; Hirschmann *et al.*, 1999; Walter, 1999; Asimow *et al.*, 2001) and physical mechanisms of melt extraction and delivery to the very narrow axial zone of crustal accretion (e.g. Phipps Morgan, 1987; Sparks & Parmentier, 1991; Spiegelman & Kenyon, 1992; Spiegelman & Elliot, 1993; Kelemen *et al.*, 1995, 1997; Lundstrom *et al.*, 1995; Niu *et al.*, 1996; Niu, 1997; Forsyth *et al.*, 1998; Asimow, 1999; Lundstrom, 2000; Spiegelman *et al.*, 2001) remain somewhat elusive. Geophysical and theoretical approaches (e.g. Spiegelman, 1993; Aharonov *et al.*, 1997; Toomey *et al.*, 1998; Spiegelman *et al.*, 2001) are useful, but the petrology and geochemistry of the melting products still provide most of the primary information. Current petrological and geochemical interpretations in these respects are, however, unconstrained. For example, to reveal details of mantle melting processes from studying MORB alone is not straightforward. Calculated melting parameters such as the extent and depth of melting from MORB compositions (e.g. Klein & Langmuir, 1987; Niu & Batiza, 1991; Kinzler & Grove, 1992; Langmuir *et al.*, 1992) are arguably invalid if the mantle source composition proves to be heterogeneous on all scales (e.g. Natland, 1989; Albarède, 1992; Niu *et al.*, 1996, 1999, 2001, 2002*a*; Niu, 1997). To use MORB composition as a proxy for igneous ocean crust in models of chemical geodynamics (e.g. Hofmann, 1988) neglects the fact that MORB represent only a compositional end-member and constitute no more than ~10–15% of the total crustal mass (e.g. Niu, 1997; Niu *et al.*, 2002*b*; Niu & O'Hara, 2003). The uncertainties in using MORB compositions to infer primary mantle melts are beyond evaluation without a clear knowledge of melt compositional change during its ascent through the mantle (O'Hara, 1985, 1995, 1998; Kelemen *et al.*, 1997; Niu, 1997; Lundstrom, 2000; Spiegelman *et al.*, 2001; O'Hara & Herzberg, 2002) and during rather complex magma chamber processes at ocean ridges (e.g. O'Hara, 1977; O'Hara & Mathews, 1981; Langmuir, 1989; Nielson, 1989; Batiza & Niu, 1992; Sinton & Detrick, 1992; O'Hara & Fry, 1996; Korenaga & Kelemen, 1997; O'Hara & Herzberg, 2002) as revealed in drill cores of oceanic lower-crustal gabbros (e.g. Dick *et al.*, 2000, 2002; Natland & Dick, 2001; Niu *et al.*, 2002*b*).

Abyssal peridotites, the mantle materials as such, should provide more direct information on mantle melting, melt extraction and post-melting processes. Indeed, Dick *et al.* (1984) not only established that abyssal peridotites are mantle melting residues for MORB, but also demonstrated, using primary mineral modes and compositions of these peridotites, that the extent of mantle melting is high beneath hotspot-influenced shallow ridges, and is low beneath deep ridges away from hotspots (also see Dick & Fisher, 1984; Michael & Bonatti, 1985). Johnson *et al.* (1990) argued that the trace element systematics of residual clinopyroxene (cpx) in abyssal peridotites results from perfect or near-perfect fractional melting. This latter argument has been widely used as the strongest evidence in support of fractional melting models for MORB genesis (e.g. Grove *et al.*, 1992; Langmuir *et al.*, 1992; Spiegelman & Kenyon, 1992; Turcotte & Phipps Morgan, 1992). Recent abyssal peridotite studies (Niu, 1997; Niu *et al.*, 1997) confirmed the melt–residue complementarity between MORB and abyssal peridotites, but also revealed the hidden complexities in these peridotites such as olivine addition and melt refertilization (also see Elthon, 1992; Niu & Hekinian, 1997*b*). These same studies (Niu, 1997; Niu *et al.*, 1997) immediately excited heated debates on the petrogenesis of abyssal peridotites (Asimow, 1999; Baker & Beckett, 1999; Niu, 1999, 2003, submitted; Walter, 1999; Lundstrom, 2000). Although such debates are useful for conceptual clarifications, a genuine understanding of the petrogenesis of abyssal peridotites remains out of reach because we do not have sufficient observations. For example, everything that has been said so far about abyssal peridotites in the literature, including those severe debates, is largely based on the same limited observations: modes and major element compositions of residual minerals, and some trace element data on residual cpx (Dick *et al.*, 1984; Dick,

1989; Johnson *et al.*, 1990). Bulk-rock major and trace element data on a small sample suite from the Garrett Transform in the Pacific (Niu & Hekinian, 1997*b*), which hinted at some surprises, have been overlooked, because they may be local phenomena with no global significance and because the scientific community has always been skeptical about the bulk-rock compositions of serpentinized peridotites.

In this paper, I report bulk-rock major and trace element analyses on ~130 serpentinized abyssal peridotite samples from ridge–transform systems in the Pacific and Indian oceans. Apart from the small dataset from the Garrett Transform (Niu & Hékinian, 1997*b*), the data presented here are the first, largest and most comprehensive elemental dataset on abyssal peridotites thus far available. The samples analyzed also include those previously studied for residual cpx trace elements by ion probe (Johnson *et al.*, 1990; Johnson & Dick, 1992). These new data are surprising because (1) they cannot be explained by serpentinization or seafloor weathering; (2) they cannot be predicted from residual cpx compositions; (3) they are inconsistent with our mainstream models of mantle melting and melt extraction processes beneath ocean ridges; (4) both the abundances and systematics of many trace elements, particularly the high field strength elements (HFSE), cannot be readily explained with our present knowledge. Hence, the new data present us with an unprecedented opportunity to understand how the mantle works beneath ocean ridges in particular, and perhaps mantle dynamics in general. These data and their implications need to be considered in future models of mantle melting, melt extraction and post-melting processes beneath ocean ridges and models of chemical geodynamics.

The data presentation and discussion are organized as follows: (1) a brief description of the samples; (2) analytical methods and data; (3) a working model framework; (4) data and interpretations; (5) discussion: problems, solutions and hypotheses to be tested. All the interpretations presented here reflect the degrees to which I understand the first-order systematics of the entire dataset. No interpretations on details are attempted beyond data precision. My 'understanding' of each aspect of the data represents the best 'choice' among several conceivable possibilities. By no means do I claim that any of my preferred interpretations are correct at this stage, but I do mean to be objective and do advocate objectiveness. Alternative interpretations, so long as they are consistent with simple physics and other observations, are welcome.

SAMPLES

Roger Hékinian (formerly IFREMER, France), Bob Fisher [Scripps Institution of Oceanography (SIO), USA], Henry Dick (Woods Hole Oceanographic Institution, USA) and Pat Castillo (SIO, USA) have generously provided me with ~200 abyssal peridotite samples collected over the years from the Pacific, Indian and Atlantic ocean ridge–transform systems. These samples are highly (>60 vol. %) or entirely serpentinized. About 10 harzburgitic samples from the Garrett Transform were previously studied for both bulk-rock major and trace elements (Niu & Hékinian, 1997*b*). Of the rest of the samples, ~130 have been analyzed so far for bulk-rock major and trace elements. These samples are specifically from the Pacific–Antarctic Ridge–transform systems in the southern Pacific (see Castillo *et al.*, 1998), Central Indian Ridge–transform systems (Engel & Fisher, 1969, 1975), Southwest Indian Ridge–transform systems (Fisher *et al.*, 1987; Dick, 1989; Johnson *et al.*, 1990), and American–Antarctic Ridge–transform systems (Dick, 1989; Johnson *et al.*, 1990) in the Indian Ocean. The petrography, mineral modal data and mineral compositions for most of these samples have been previously described and published by the above workers except for samples from the Pacific–Antarctic Ridge, whose detailed petrography, not particularly different from other sample suites (partially or entirely serpentinized), will be discussed separately. Sample size is generally small, varying in weight from 20 to 200 g. The material available for analysis is even less after making standard (30 μm thick) thin-sections for petrography and 'thick' (~100 μm) 'thin-sections' for future laser-ablation inductively coupled plasma mass spectrometry (LA-ICP-MS) analysis. Given the coarse grain size, even though partially or entirely serpentinized, the small sample size explains at least partly the geochemical scatter because of the modal heterogeneity at the scale of the sample size. Nevertheless, the first-order compositional trends defined by the elemental data are still revealing (see below).

ANALYTICAL METHODS AND DATA

All samples are fresh cuttings away from late veinlets (metamorphic or magmatic impregnation, etc.) and were thoroughly cleaned. Pen marks, saw marks, sticker residues, and other suspicious surface contaminants were ground off all samples. The samples were then reduced to 1–2 cm size using a percussion mill with minimal powder production. These centimeter-size rock pieces were then ultrasonically cleaned in Mili-Q water, dried, and powdered in a thoroughly cleaned agate mill in the clean laboratory at The University of Queensland (UQ). Sample powders in ultraclean vials were placed in a clean furnace at 110°C overnight before being weighed and acid digested. Because of small sample size, preciousness of the sample material, and to avoid contaminations, no traditional 'loss on ignitions' were made on these samples.

Bulk-rock major element oxides (SiO_2, TiO_2, Al_2O_3, FeO, MnO, MgO, CaO, Na_2O, K_2O, and P_2O_5) were analyzed using a Perkin Elmer Optima 3300 DV inductively coupled plasma-optical emission spectroscopy (ICP-OES) system at UQ following the procedure of Kwiecien (1990) and Fang & Niu (2003). Precisions (1σ) on serpentinized peridotites were determined on repeated analyses of French CNRS Georeference standard UB-U with means, standard deviations (1σ) and RSD% ($= 1\sigma$/Mean $\times$ 100%) given in the last columns of Electronic Appendix 1 (downloadable from the *Journal of Petrology* website at http://www.petrology.oupjournals.org), which are close to or better than the certified working values. The data are presented in Electronic Appendix 1 on an anhydrous basis.

Bulk-rock minor and trace element (Li, Be, Sc, Ti, V, Cr, Co, Ni, Cu, Zn, Ga, Rb, Sr, Y, Zr, Nb, Cs, Ba, La, Ce, Pr, Nd, Sm, Eu, Gd, Tb, Dy, Ho, Er, Tm, Yb, Lu, Hf, Ta, Pb, Th and U) abundances in these same samples were analyzed by ICP-MS on a Fisons $PQ2^+$ system at UQ with analytical conditions and procedures following Eggins *et al.* (1997) and Niu & Batiza (1997) except for sample digestion, which was done using high-pressure bombs to ensure complete digestion/dissolution (Niu *et al.*, 2002*b*). Some samples were digested and analyzed more than once or twice, and the reported values are reproducible within analytical uncertainties. The analytical precisions (1σ) were determined by repeated analyses of USGS Georeference rock standard PCC-1 (peridotite). The means, standard deviations (1σ) and RSD% are given in the last columns of Electronic Appendix 1. Given the ultra-low abundances of many of these elements, precisions $<20\%$ are considered good (i.e. precise enough not to affect interpretations of first-order systematics). It should be noted that there are no agreed 'certified' working values yet available for all the elements of interests (analyzed) for PCC-1. The UQ PCC-1 values are given such that interested readers may wish to compare the datasets presented here with their own peridotite analyses.

A WORKING FRAMEWORK

This paper is not intended to discuss the petrogenesis of a particular sample or sample suite from a particular ridge–transform system, but to discuss first-order implications of the data as a whole assuming they are of a global significance. Therefore, a general working framework is useful for data interpretations. Figure 1 presents such an ideal framework, which is modified from Niu (1997), for mantle melting, melt extraction and post-melting processes beneath ocean ridges. This model framework states the following: (1) plate separation at ocean ridges causes the asthenospheric mantle below to rise; (2) this rising mantle begins to melt when it intersects the solidus at a depth P_o; (3) melting continues as the melting mantle rises (decompression) until it reaches a depth P_f as a result of conductive cooling to the seafloor; (4) the depth range between the base of the igneous crust and the depth of melting cessation (P_f) is termed 'cold' thermal boundary layer (TBL; grey region and thick blue lines with arrows indicating the solid mantle flow field); (5) no melting occurs in the TBL, but new ascending melts (red lines with arrows) migrate through and interact with the advanced residues of previous melting in the TBL; (6) residues from the central melting column rise to the shallowest level, experience significant melt refertilization or melt–solid interaction, and undergo serpentinization before being sampled on the seafloor as abyssal peridotites; (7) on the other hand, melting residues away from the central column are likely to flow sideways at deep levels, leaving the sub-ridge magmatic system with limited melt refertilization or melt–solid interaction, and without being serpentinized; (8) the latter residues could be preserved as fresh massif or ophiolitic peridotites in the geological record, but would never be the same as abyssal peridotites; (9) this requires that caution be exercised when comparing serpentinized abyssal peridotites with fresh ophiolitic/massif peridotites even if the latter can be proved to be MORB melting residues.

DATA AND INTERPRETATIONS

Bulk-rock major elements of abyssal peridotites

Effects of serpentinization

Because previously studied abyssal peridotites (e.g. Dick & Fisher, 1984; Dick *et al.*, 1984; Michael & Bonatti, 1985; Dick, 1989; Johnson *et al.*, 1990; Johnson & Dick, 1992; Niu & Hékinian, 1997*b*) were mostly highly or entirely serpentinized, and because of the common knowledge that serpentinization would obliterate the magmatic signatures recorded in the compositions of the peridotites, major element analyses of bulk-rock abyssal peridotites have never been considered useful for understanding pre-serpentinization processes. For this reason, and to characterize melting processes from 'melting residues', Niu *et al.* (1997) attempted to reconstruct what bulk-rock compositions abyssal peridotites would have prior to serpentinization using mineral chemical data and estimated primary mineral modes (e.g. Dick, 1989). Niu's (1997) quantitative treatment of the reconstructed data has revealed a number of intriguing phenomena concerning mantle melting and melt extraction processes. The latter and Niu *et al.* (1997) have also excited heated debates (Asimow, 1999; Baker & Beckett, 1999; Niu, 1999, 2003, submitted; Walter, 1999; Lundstrom, 2000).

Figure 2a illustrates the bulk-rock chemical variation of the studied abyssal peridotites in MgO/SiO_2–Al_2O_3/SiO_2 space. Reconstructed bulk-rock compositions from

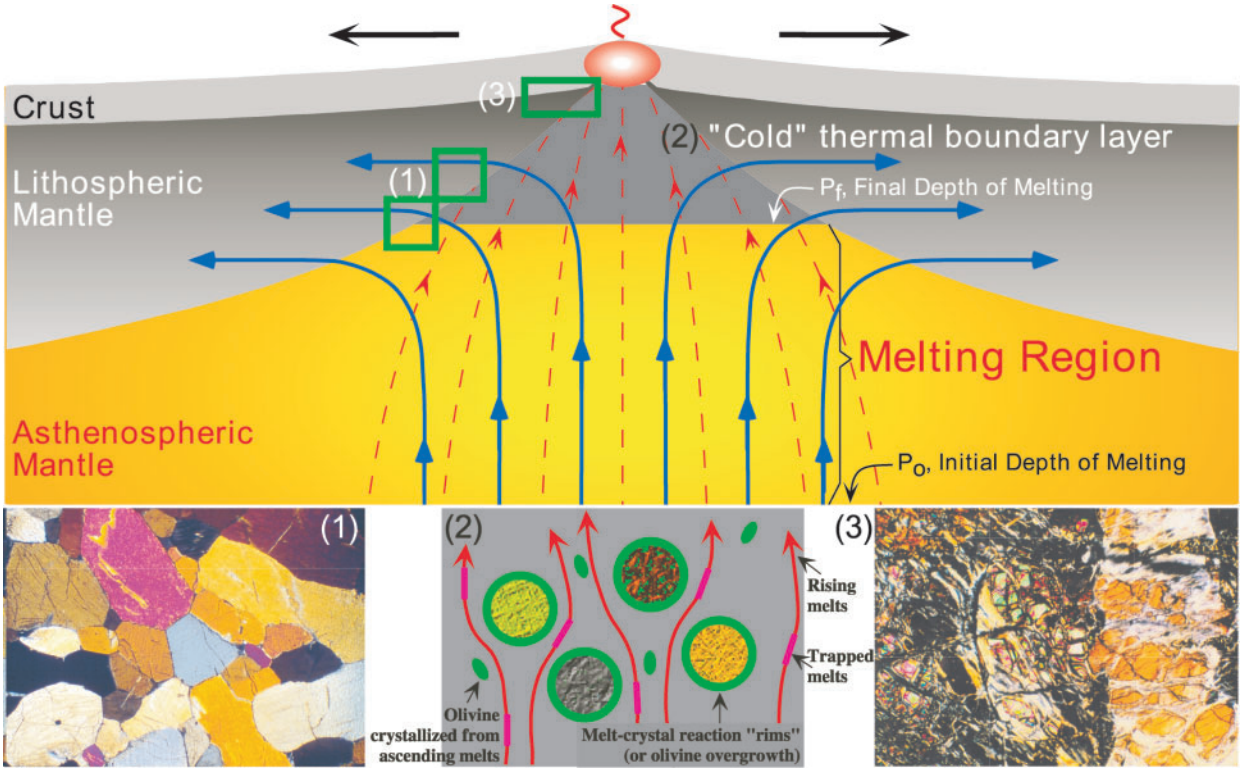

Fig. 1. A working framework for interpreting the geochemical characteristics of abyssal peridotites in the context of mantle melting, melt extraction and post-melting processes beneath mid-ocean ridges (modified from Niu, 1997). The mantle beneath an ocean ridge is conveniently considered as having two regions: the melting region between the solidus (P_o) and the depth of melting cessation (P_f) as a result of conductive cooling to the seafloor, and the cold thermal boundary layer (TBL, labeled '2') between the base of the crust and P_f. No melting occurs in the TBL, but the advanced residues continue to rise and flow laterally away from the ridge (thick arrowed lines). The newly formed melts at depth ascend, migrate through and interact with advanced residues in the TBL, including cooling-induced olivine crystallization, entrapment of melt, and complex 'chromatographic' processes. The advanced residues so processed, particularly in the central column of the TBL, continue to rise to shallow levels and are variably serpentinized (labeled '3') before they are tectonically exposed and sampled on the seafloor as abyssal peridotites. On the other hand, melting residues at deep levels (labeled '1') that turn laterally will not experience the TBL processes, never be serpentinized, and never be sampled as abyssal peridotites, but may be sampled as fresh ophiolitic or massif peridotites in the geological record (e.g. Frey *et al.*, 1985; Godard *et al.*, 2000; Griselin & Davies, 2003).

Niu *et al.* (1997) and the so-called 'terrestrial array' (Jagoutz *et al.*, 1979; Hart & Zindler, 1986) are also plotted for comparison. The 'terrestrial array' is in fact a magmatic depletion (or enrichment) trend from a primitive mantle of $MgO/SiO_2 \sim 0{\cdot}85$ and $Al_2O_3/SiO_2 \sim 0{\cdot}1$ (lower right) to highly depleted harzburgitic composition of $MgO/SiO_2 \sim 1{\cdot}1$ and $Al_2O_3/SiO_2 \sim 0$ (upper left). The fact that the reconstructed bulk compositions of abyssal peridotites from Niu *et al.* (1997) plot in the same position and with identical slope to the 'terrestrial array' corroborates the validity of the reconstructed bulk compositions. The actual bulk-rock analyses of most of the studied samples plot below the terrestrial array. The best, not necessarily unique or correct, explanation is that the serpentinized peridotites are generally depleted in MgO. Such depletion is probably due to seafloor weathering (Snow & Dick, 1995) rather than serpentinization (see below). The scatter is probably caused mostly by the compositional heterogeneity and small size of samples analyzed as well as varying degrees of weathering. However, the statistically significant (at >99·9% confidence levels) negative trend ($R = -0{\cdot}629$) with a slope ($-2{\cdot}596$) identical to that of the terrestrial array ($-2{\cdot}598$) is somewhat surprising. If we assume SiO_2 and Al_2O_3 are both immobile during serpentinization, then the mean MgO loss or depletion with respect to SiO_2 is, to a first order, ~10% (note the intercept of 1·019 vs 1·107, which is ~10% relative difference in MgO). Such a mean value of ~10% relative MgO loss (i.e. 10% of the total MgO in the protoliths) should be close to the actual loss because of the common denominator (SiO_2) on this ratio–ratio plot that is independent of analytical totals (i.e. the effect of 'loss on ignition'). Given that the relative ease of serpentinization is in the order of olivine > orthopyroxene (opx) > cpx, which is consistent with the order of relative abundances of these minerals in fresh peridotites, we can safely say that the mean 10% relative MgO loss is mostly due to contribution of serpentine after olivine

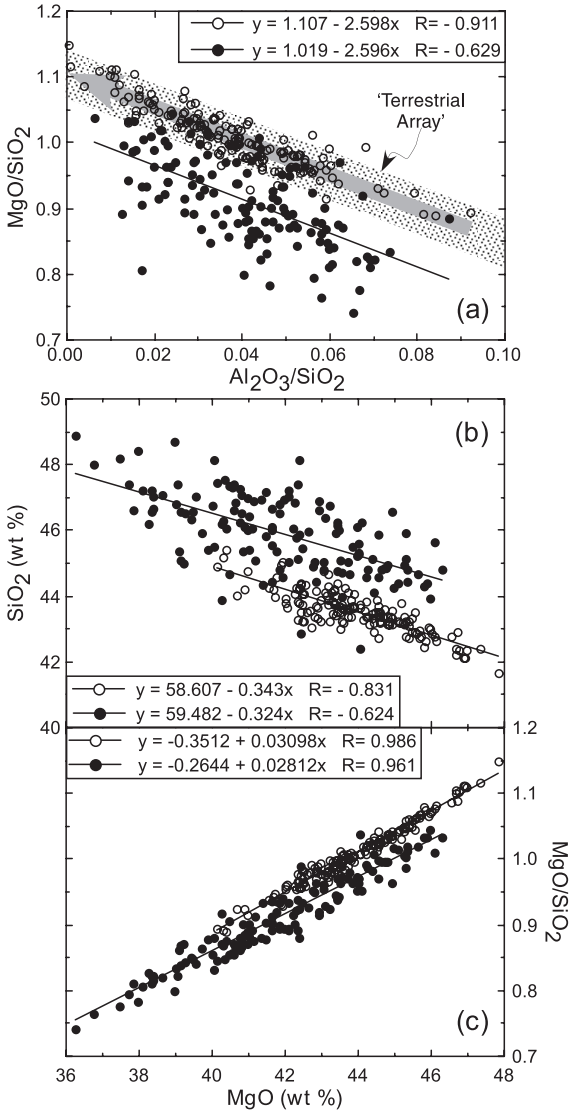

Fig. 2. Comparisons between actual bulk-rock analyses (filled circles; normalized to 100% anhydrous totals) and reconstructed bulk-rock compositions (Niu *et al.*, 1997) of abyssal peridotites (open circles). (a) In MgO/SiO_2–Al_2O_3/SiO_2 space, the reconstructed bulk compositions define a tight trend ($R = -0{\cdot}911$, indicated by the thick gray line with arrow) that is identical to the 'terrestrial array' (Jagoutz *et al.*, 1979; Hart & Zindler, 1986). The scattered, yet statistically significant trend ($R = -0{\cdot}629$) defined by the analyzed bulk compositions gives a slope ($-2{\cdot}596$) identical to the slope of the terrestrial array ($-2{\cdot}598$), but about 10% lower (i.e. 1·019 vs 1·107 in their respective intercepts) in MgO/SiO_2 at a given Al_2O_3/SiO_2. (b) in SiO_2–MgO space, both datasets define negative trends with essentially identical slopes ($-0{\cdot}343$ and $-0{\cdot}324$, respectively). (c) in MgO/SiO_2–MgO space, both datasets show similar slopes and very tight trends, indicating that the magmatic signatures in these serpentinized and weathered abyssal peridotites remain preserved.

(note that MgO loss during seafloor weathering mostly results from serpentines, not primary olivine crystals) whereas the scatter about the 10% mean may be due to the 'contributions' of opx and cpx, whose modal abundances are variable from one sample to another because of the small sample size studied. Post-melting magmatic refertilization (see below) could also contribute to the lowered MgO/SiO_2 ratios in abyssal peridotites but that effect is likely to be small. All the above analysis suggests that, to a first order, bulk-rock MgO values still retain some magmatic signals such as the extent of melting or melt depletion [proportional to modal olivine/(opx + cpx) ratios]; most samples have lost some MgO, with a mean of ~10 relative wt %, which seems to be independent of the actual MgO contents of the unserpentinized protoliths.

Figure 2b compares bulk-rock analyses with reconstructed bulk-rock compositions of abyssal peridotites in SiO_2–MgO space. The statistically significant negative trends with essentially the same slopes defined by both datasets ($-0{\cdot}324$ vs $-0{\cdot}343$) suggest that the pre-serpentinization magmatic signatures are retained in actual bulk-rock analyses. This is also clear from MgO/SiO_2–MgO plot of Fig. 2c. The high SiO_2 values of the actual analyses probably result from renormalization to 100 wt % on an anhydrous basis. By adding ~10 wt % relative MgO and renormalizing the bulk-rock analyses to 100 wt %, the actual data overlap reasonably well with the reconstructed bulk-rock compositions. Figure 2b and c also suggests that the low MgO/SiO_2 ratios of actual bulk-rock analyses in Fig. 2a are due not to SiO_2 addition, but to MgO depletion. It should be noted also that the mean Mg-number, Mg/(Mg + Fe), of the dataset based on actual analyses is $0{\cdot}8956 \pm 0{\cdot}0131$, which is low, whereas the mean Mg-number $= 0{\cdot}9042 \pm 0{\cdot}0121$ after 10% relative MgO addition. The latter is expected and is similar to the reconstructed bulk-rock mean value of $0{\cdot}9022 \pm 0{\cdot}003$ (Niu *et al.*, 1997). It should be noted that this result is not due to Fe addition, but MgO loss. The few samples with elevated FeO in Fig. 3d are from the Garrett Transform and result from impregnation of highly evolved melts (see Niu & Hekinian, 1997*b*, fig. 3).

MgO variation diagrams and implications

Figure 3 compares actual bulk-rock analyses with reconstructed bulk compositions of abyssal peridotites on MgO variation diagrams for SiO_2, TiO_2, Al_2O_3, FeO, CaO and Na_2O. For reference, the isobaric and polybaric melting models of Niu (1997) are also shown. All the analyses are plotted on an anhydrous basis. As discussed above, by adding ~10% relative MgO, and renormalizing the bulk analyses to 100 wt %, the bulk-rock analyses will shift and overlap significantly with the reconstructed bulk-rock compositions. In this case, the interpretations of major element systematics are essentially the same as those given by Niu (1997). The bulk trends on CaO–MgO and Al_2O_3–MgO plots can be explained by varying degrees of melt depletion by either isobaric batch melting

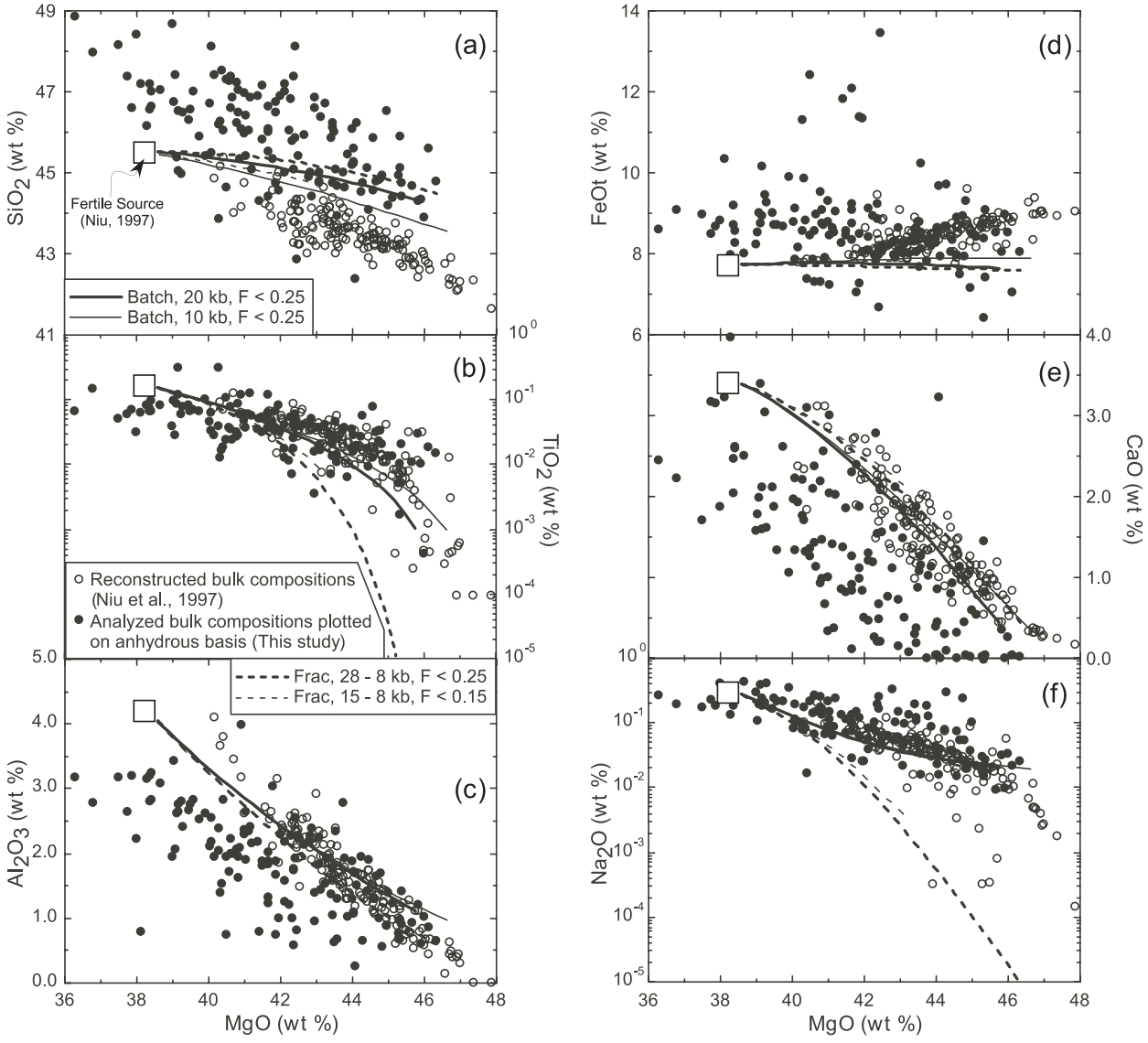

Fig. 3. Comparisons between actually analyzed and reconstructed bulk compositions of abyssal peridotites (same symbols as in Fig. 2) on MgO variation diagrams vs SiO_2 (a), TiO_2 (b), Al_2O_3 (c), FeOt (d), CaO (e) and Na_2O (f). For comparison, also plotted are calculated melting residues of both isobaric batch melting (at $P = 10$ and 20 kbar, respectively) and near-fractional (1% melt porosity) decompression melting (28–8 kbar and 15–8 kbar, respectively) models of Niu (1997). Considering the probably ~10% relative MgO (~10% of MgO in the protoliths) loss in analyzed abyssal peridotites (see text), the Al_2O_3–MgO and CaO–MgO trends can be explained by both melting models. The TiO_2–MgO and Na_2O–MgO trends are better explained by batch (vs near-fractional melting) melting. To a first order, the Niu (1997) and Niu *et al.* (1997) interpretation for SiO_2–MgO and FeOt–MgO trends remains valid despite the current debate (see text). The scatter and large variation in FeOt–MgO space largely results from inhomogeneous distribution of 'FeOt' in serpentinized peridotites and the small size of the samples studied.

or near-fractional polybaric melting. To show the details, both TiO_2 and Na_2O are plotted on logarithmic scales. Obviously, batch melting can better explain TiO_2–MgO and Na_2O–MgO trends than fractional melting, which contrasts with interpretations based on residual cpx trace element data (Johnson *et al.*, 1990).

The negative SiO_2–MgO trend and the FeO–MgO scattering cannot be readily explained by either melting model. For the reconstructed bulk compositions, the steep negative SiO_2–MgO trend and the positive FeO–MgO trend were interpreted by Niu (1997) and Niu *et al.* (1997) as resulting from olivine addition in the cold TBL atop the mantle beneath mid-ocean ridges (see Fig. 1) because excess olivine exists in the original modal data (e.g. Dick, 1989; Johnson *et al.*, 1990; Niu, 2003, submitted), and because the trends indeed point to the mean composition of olivine, with high FeO, high MgO and low SiO_2. Baker & Beckett (1999) argued that the Niu *et al.* (1997) interpretation was an artifact of their incorrect bulk composition reconstructions, and that no

positive FeO–MgO correlation should exist in 'properly' reconstructed bulk compositions (Griselin & Davies, 2003). The fact that compared with the expected melting residues (Niu *et al.*, 1997), excess olivine is evident in abyssal peridotite modal data (Dick, 1989; Niu & Hékinian, 1997*b*), the positive FeO–MgO trend in reconstructed bulk compositions of abyssal peridotites is the consequence of, not evidence for, excess olivine in these rocks [see Niu (2003, submitted) for details]. If we add ~10% relative MgO (i.e. MgO × 110%), and renormalize the bulk analyses to 100 wt %, over two-thirds of the data points will lie on the positive FeO–MgO trend defined by the reconstructed bulk compositions. The few very high FeO samples are from the Garrett Transform (Niu & Hékinian, 1997*b*). The question is how to explain the rest of the samples that have both higher and lower FeO than the main trend and the model melting curves. Petrographic studies suggest that such scatter results from the heterogeneous distribution of 'FeO' in abyssal peridotites. This is because serpentinization forms Fe-poor serpentines by concentrating Fe (mostly as fine-grained aggregates of magnetite) as trails away from domains of serpentine. As a result, the analyzed FeO contents in serpentinized peridotites depend on sample size and whether the sample analyzed is dominated by serpentines (Fe-poor) or by magnetite trails (Fe-rich).

Can melting systematics survive serpentinization?

Following Niu (1997), we can recast bulk-rock analyses in terms of low-pressure peridotite modes (wt %) of olivine, opx, cpx and spinel [see Niu (1997, appendix C and fig. 5)]. Figure 4a plots such calculated modes against bulk-rock MgO. Despite some minor differences, the 'modes' derived from actual bulk-rock analyses (large symbols) are remarkably similar to observed 'modes' (small symbols; Dick, 1989) for which MgO is calculated from reconstructed bulk-rock compositions (Niu, 1997). This demonstrates that although abyssal peridotites undoubtedly have experienced some MgO loss and probably other changes, the original melting systematics remain largely preserved in highly serpentinized peridotites. This is unexpected given the widespread belief that serpentinization obliterates the magmatic signatures in peridotites (e.g. Dick *et al.*, 1984; Michael & Bonatti, 1985; Dick, 1989; Johnson *et al.*, 1990; Elthon, 1992; Niu *et al.*, 1997). The slight differences are readily explained by the differences in analyzed bulk-rock compositions. For example, the low MgO (MgO loss; see above) and apparent high SiO_2 (effect of normalization to anhydrous totals of 100 wt %) in actual analyses of bulk-rock compositions can explain the relatively low olivine and high opx modes.

Figure 4b plots mass fractions of calculated mineral modes from bulk-rock analyses as a function of F, where

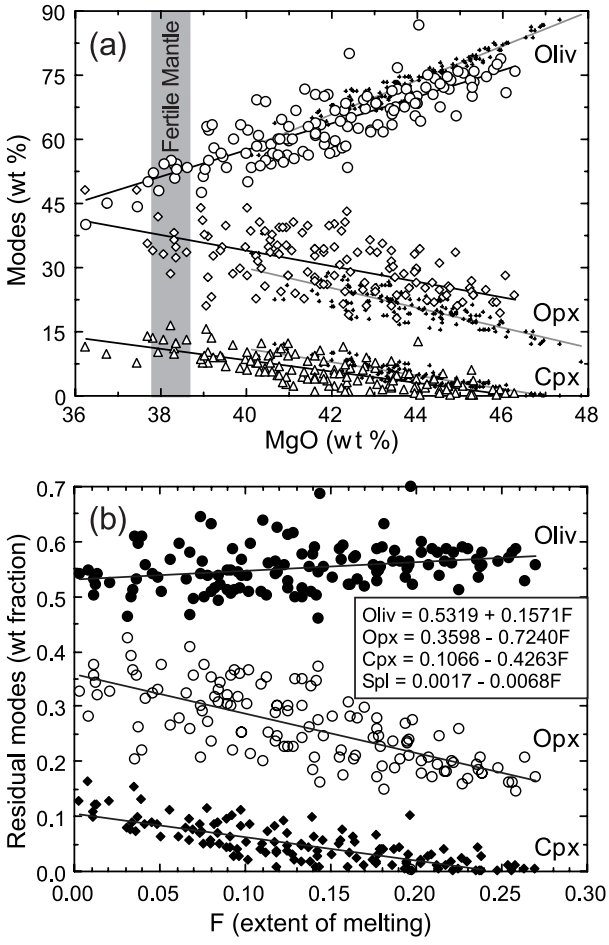

Fig. 4. (a) Comparisons between observed modes of olivine, opx and cpx (wt %; small symbols) in abyssal peridotites (Dick, 1989; Niu *et al.*, 1997) with those calculated (Niu, 1997) from actually analyzed bulk compositions of abyssal peridotites (large symbols) on MgO variation diagrams. (b) Plot of the results in (a) in terms of modal mass fractions (normalized to a total of $1 - F$) against the extent of melting (F) to show that the incongruent melting relationship derived from the actually analyzed serpentinized samples [−0·4263 Cpx −0·7240 Opx −0·0068 Spinel +0·1571 Olivine +1·0000 Melt = 0] resembles remarkably that derived from the actual modes [−0·466 Cpx −0·652 Opx −0·049 Spinel +0·167 Olivine +1·000 Melt = 0] (Niu, 1997, 1999). Particularly noteworthy are the consistent opx/cpx >1 ratios interpreted to characterize decompression melting (Niu, 1997). For comparison purpose, the extent of melting (F) is calculated using a single fertile mantle source (MgO = 38·3 ± 0·53 wt%): $F = -1{\cdot}234 + 3{\cdot}249 \times 10^{-2}$ MgO (Niu, 1997). The calculated F values should not be taken as having true significance, but the consistent melting relationship in both (a) and (b) indicates that serpentinization and weathering did not obliterate magmatic signatures in these rocks.

F represents the mass fraction of melt extraction from a model source. Except for spinel, the systematic trends defined by olivine, opx and cpx modes give a melting relationship very close to the polybaric melting relationship derived from original modes (e.g. Dick, 1989) after correction for olivine addition (Niu, 1997); opx contributes more than cpx to melts produced by decompression melting

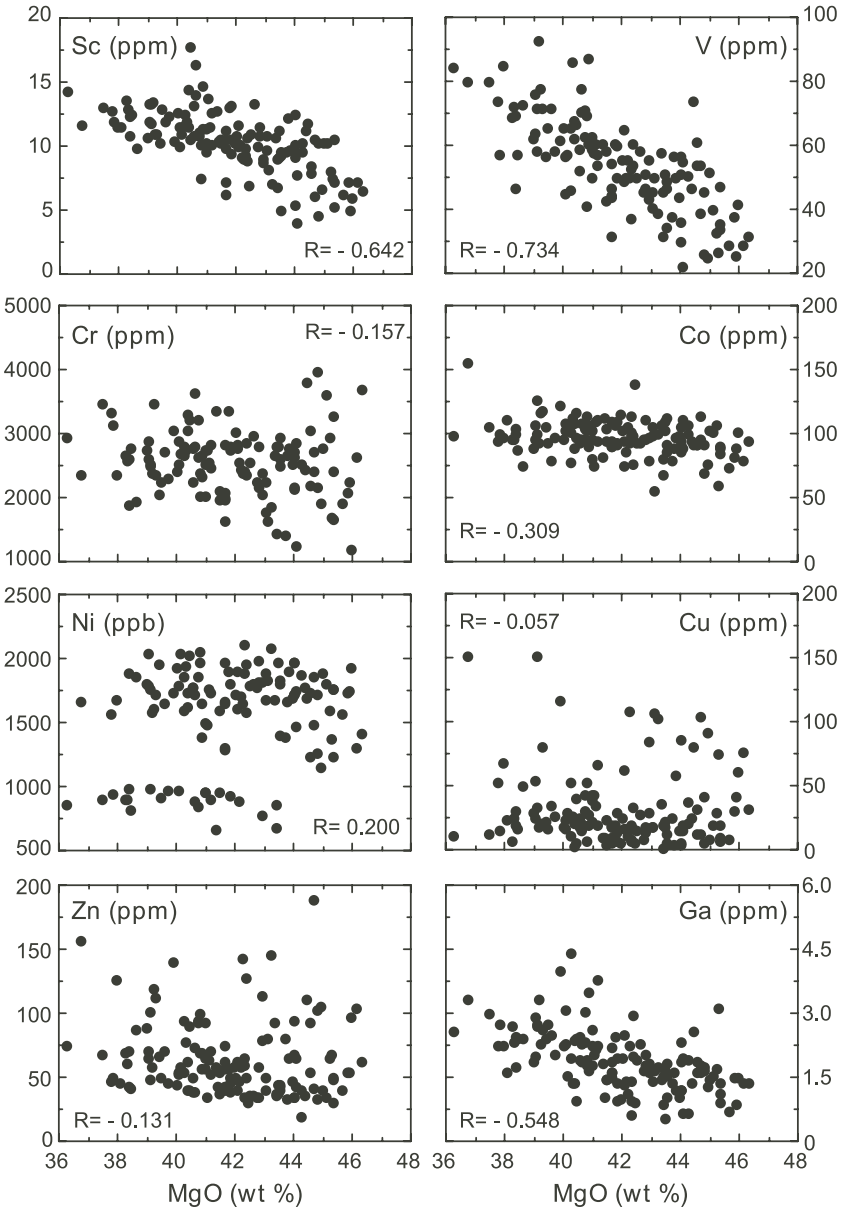

Fig. 5. MgO variation diagrams of representative transition metals plus Ga (see text for details).

[Niu, 1997, figs 6, 7 and 12, and equation (8)]. Again, despite the compositional alteration during serpentinization and seafloor weathering, these late-stage, low-temperature, processes have not obliterated the magmatic systematics of the protoliths prior to serpentinization.

Bulk-rock minor and trace elements of abyssal peridotites

Transition metals plus gallium

Figure 5 illustrates the variation of a range of transition metals plus Ga against MgO. The statistically significant negative trends of Sc–MgO, V–MgO and Ga–MgO are expected because these elements are mildly incompatible during mantle melting. If these trends reflect recent sub-ridge melting processes, then they suggest that MORB melts are mostly generated in the spinel (vs garnet) peridotite stability field (e.g. Niu & Batiza, 1991; Niu, 1997) as Sc is highly compatible in garnet and the negative Sc–MgO trend would not exist otherwise. The slope of V–MgO is consistent with a MORB mantle oxygen fugacity between QFM – 3 and QFM – 1 (where QFM is the quartz–fayalite–magnetite buffer) (Wood *et al.*, 1990; Lee *et al.*, 2003). These observations also suggest that Sc,

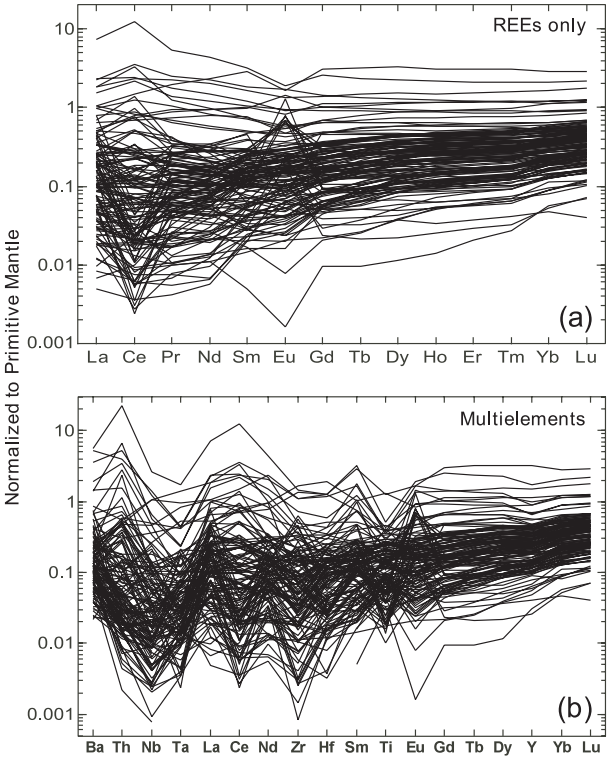

Fig. 6. Primitive mantle (Sun & McDonough, 1989) normalized REE patterns (a) and selected multi-element diagram (b) of bulk-rock abyssal peridotites to show the non-smooth patterns and over 2–3 orders of magnitude abundance variations, suggesting that abyssal peridotites are not simple residues (Niu & Hékinian, 1997*b*; Niu *et al.*, 1997) but have experienced significant post-melting modifications.

V and Ga are more or less immobile or unaffected by serpentinization and seafloor weathering. The flat and slightly negative Co–MgO trend is consistent with Co having a bulk distribution coefficient close to unity, and also suggests that Co is immobile during serpentinization. The apparent scatter of Cu, Zn, Ni and Cr does not necessarily mean these elements are mobile during serpentinization, but may suggest formation of minor phases whose distribution is heterogeneous on the scale of the small sample size. Chromite (Cr, Zn, Fe), sulfides (Cu, Ni, Fe), native metal/alloys (Ni, Co, Fe) are probably the responsible phases, readily seen by scanning electron microscopy (SEM). The ubiquitous magnetite also incorporates some Zn.

Rare earth and other incompatible trace elements

Figure 6 shows primitive-mantle normalized bulk-rock rare earth element (REE) and multielement patterns of all the analyzed samples (Electronic Appendix 1, available for downloading from http://www.petrology.oupjournals.org) plus some analyses from the Garrett Transform (Niu & Hékinian, 1997*b*). Given the widely accepted notion that abyssal peridotites are MORB melting residues (e.g. Dick *et al.*, 1984; Johnson *et al.*, 1990), although not simple residues (Niu *et al.*, 1997), and that melting occurs as a fractional melting process (Johnson *et al.*, 1990), the over 3–4 orders of magnitude abundance variations in these incompatible elements in bulk-rock abyssal peridotites are unexpected. Given the fact that MORB melts show relatively smooth patterns on these plots, the non-smooth patterns of bulk-rock abyssal peridotites suggest these rocks experienced more complex processes. The Ce anomalies in the REE plot may suggest seawater effects, either seafloor weathering or during serpentinization involving fluids that are ultimately of seawater origin. The apparent Eu anomalies, which are often attributed to the role of plagioclase, could be due to Eu mobility (e.g. as is Sr) or to a late-stage magmatic imprint (Niu & Hékinian, 1997*b*).

Bulk-rock light REE are more enriched, not more depleted, than in the constituent residual cpx of the same sample suites

Figure 7 shows that (except for samples from the Prince Edward Transform) residual cpx in abyssal peridotites from the Southwest Indian Ridge (SWIR) and American–Antarctic Ridge (AAR) transform systems are highly depleted in light REE (LREE) with flat-to-elevated middle to heavy REE (MREE–HREE), consistent with varying extents of melt depletion through fractional melting (Johnson *et al.*, 1990). In contrast, bulk-rock data for the same sample suites show elevated abundances of LREE with flat to enriched HREE patterns. Given the fact that among all the known residual phases (olivine, opx, cpx and spinel) cpx has the highest mineral/melt partition coefficients, residual olivine, opx, and spinel in equilibrium with the cpx and with each other should have lower LREE abundances than the cpx, and therefore bulk-rock samples should have lower, not higher, LREE abundances than the cpx. Hence, the observations in Fig. 7 are entirely unexpected and emphasize that our present knowledge is yet incomplete on the petrogenesis of abyssal peridotites in the context of ocean ridge processes.

As all these peridotites are serpentinized to various extents, the elevated abundances of LREE could be due to serpentinization, a hydrothermal metamorphic process (~250–400°C with up to 13 wt % H_2O in serpentinites), during which the LREE could be mobile and added in. Average seawater has REE levels (e.g. Elderfield & Greaves, 1982) 4–6 orders of magnitude lower than in abyssal peridotites, so seawater cannot be a promising source for excess LREE in these rocks. However, seawater is the ultimate source for ridge hydrothermal fluids, which could leach LREE out of the crustal lithologies and subsequently precipitate them during serpentinization atop the mantle, giving rise to

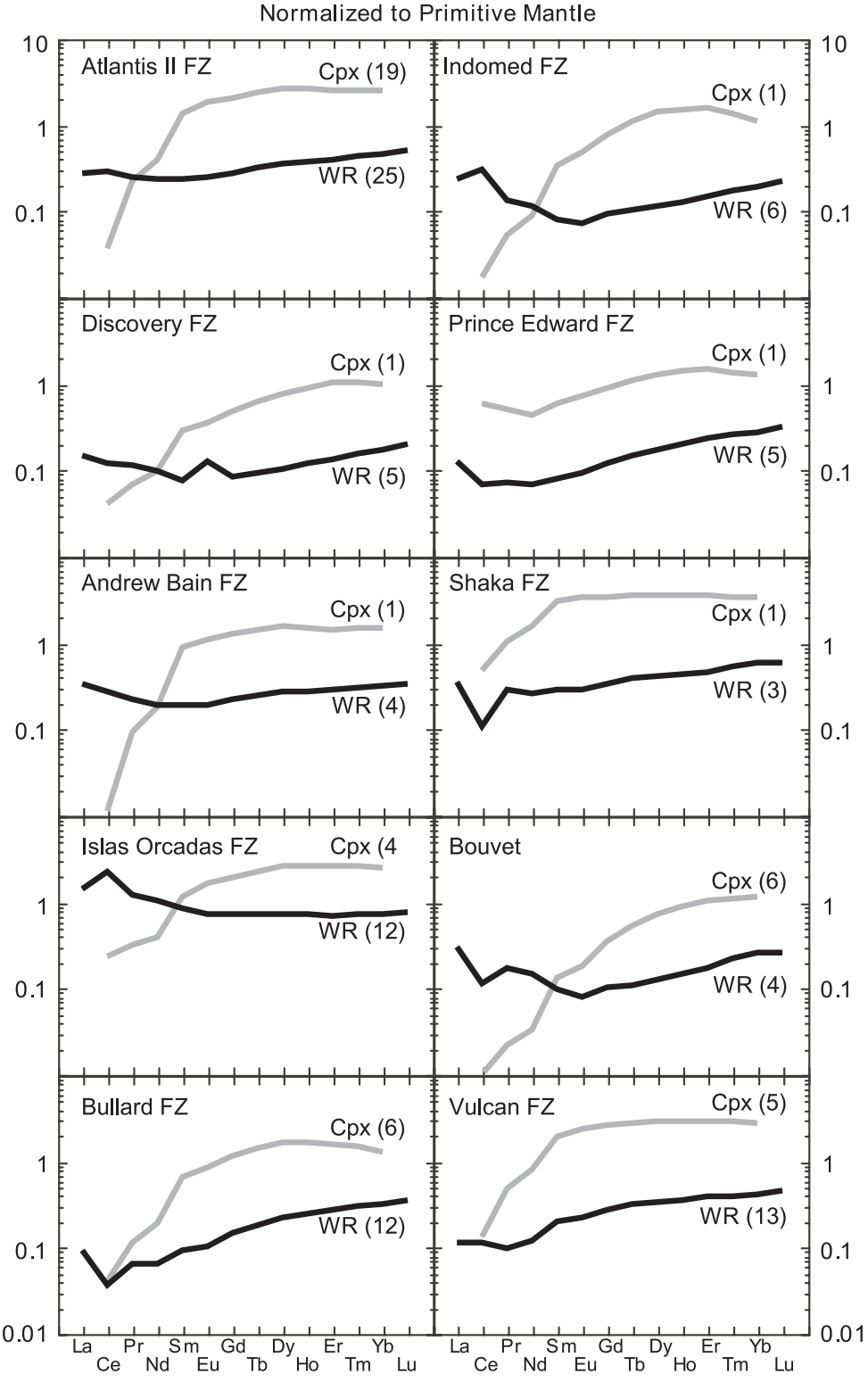

Fig. 7. Comparison of primitive mantle normalized REE contents of average residual cpx (Johnson *et al.*, 1990; Johnson & Dick, 1992) with average bulk-rock (WR) compositions of the same sample suites from ridge–transforms of the Southwest Indian and American–Antarctic ridges. Except for samples from the Prince Edward Transform, residual cpx show highly depleted LREE abundances. In contrast, bulk-rock compositions show flat or LREE-enriched patterns. The Ce anomalies may be due to seafloor weathering, but could also have been inherited from seawater, the ultimate source of hydrothermal fluids for serpentinization. The numerals in parentheses are the number of analyses available for averaging.

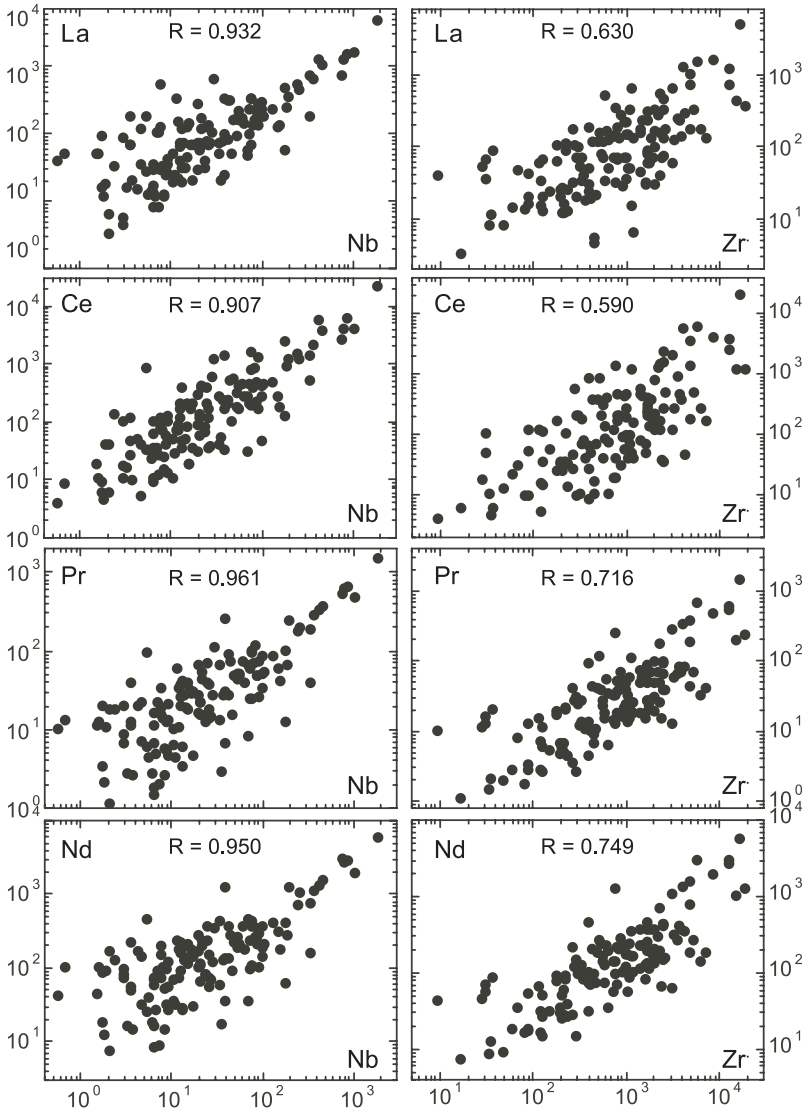

Fig. 8. The statistically significant correlations of LREE (e.g. La, Ce, Pr and Nd) with HFSE (e.g. Nb and Zr) indicate that the process or processes that led to REE enrichments also caused the HFSE enrichments.

the elevated abundances of LREE in serpentinized abyssal peridotite samples. Although this interpretation is sensible, it is, however, inconsistent with other observations.

The statistically significant (at >99·99% confidence levels for $N > 130$ samples) positive correlations of LREE with HFSE (e.g. $R_{La–Nb} = 0{\cdot}932$, $R_{Ce–Nb} = 0{\cdot}907$, $R_{Pr–Nb} = 0{\cdot}961$, $R_{Nd–Nb} = 0{\cdot}950$; $R_{La–Zr} = 0{\cdot}630$, $R_{Ce–Zr} = 0{\cdot}590$, $R_{Pr–Zr} = 0{\cdot}716$, $R_{Nd–Zr} = 0{\cdot}749$) in Fig. 8 suggest that the process or processes that led to the enrichments of LREE also led to the enrichments of HFSE such as Zr and Nb. Whereas LREE could be mobile during serpentinization, no data yet available in any form obtained by any means (e.g. observations or experiments) suggest that HFSE could be mobile during hydrothermal alteration or metamorphism. In fact, hydration/dehydration experiments (e.g. You *et al.*, 1996; Kogiso *et al.*, 1997) under both shallow and relatively deep subduction zone conditions demonstrate consistently that Nb, Ta, Zr, etc. are essentially immobile. The significant correlations between LREE and HFSE in bulk-rock abyssal peridotite samples also suggest that neither HFSE nor LREE are significantly mobile during serpentinization because otherwise we would not see the highly correlated variations (Fig. 8) but scattering or 'decoupling'. The above reasoning suggests that the elevated abundances of LREE and HFSE in bulk-rock abyssal peridotites (vs residual cpx; Fig. 7) both resulted

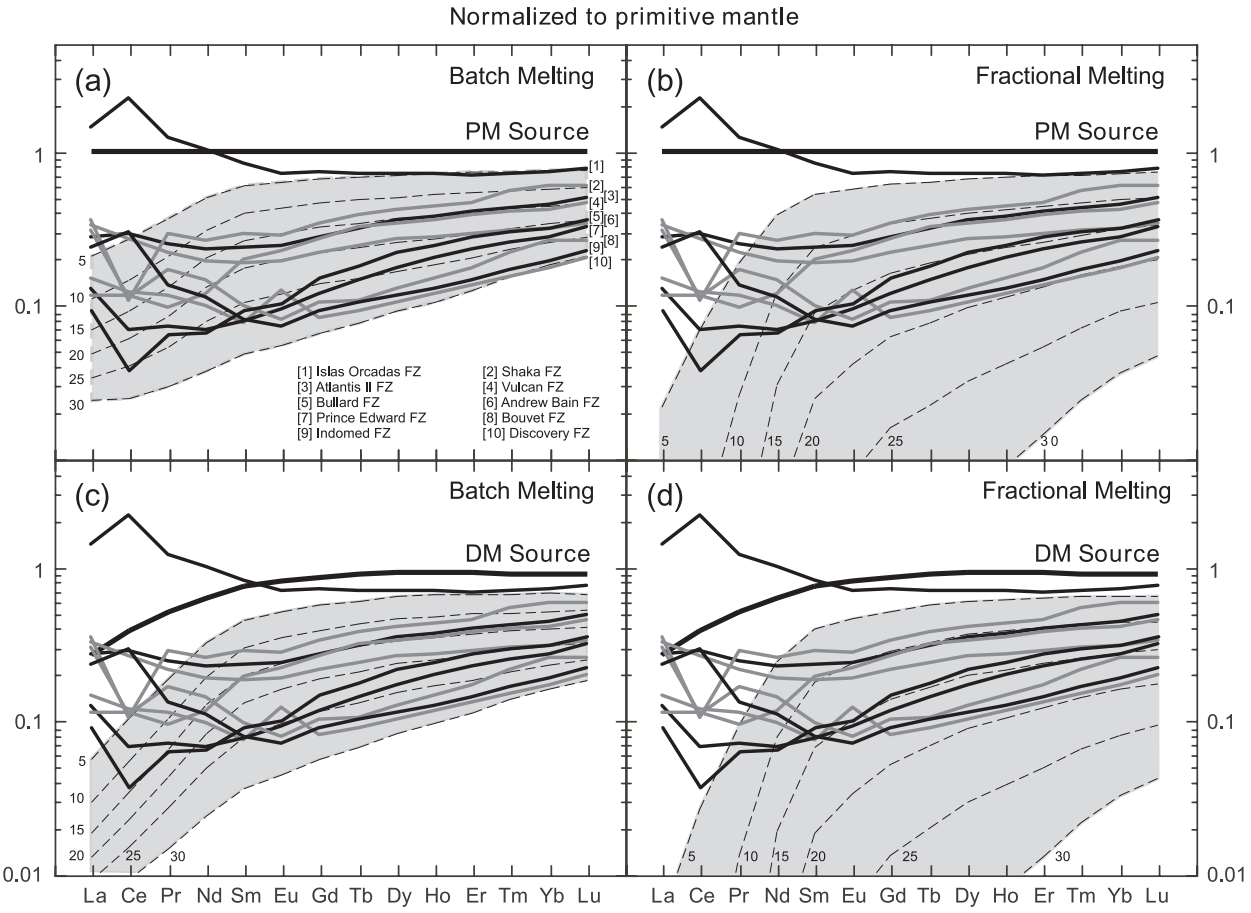

Fig. 9. Comparison of primitive mantle normalized REE patterns of abyssal peridotite site averages (Fig. 7) with endmember batch (a and c) and fractional (b and d) melting models using both primitive mantle (PM; a and b) (Sun & McDonough, 1989) and a depleted mantle source (DM; c and d) (Niu & Hékinian, 1997*b*). All the model parameters and distribution coefficients are taken from the literature and have been summarized by Niu & Hékinian (1997*b*). Except for the sample suite from the Islas Orcadas transform, the slopes of MREE and HREE (after Sm) of all sample suites can be reasonably well explained by varying extents of melting from either model using either source. However, the elevated abundances of LREE (La, Ce, Pr, Nd) cannot be explained by either melting model using either source. The shaded regions represent residues of 5–30% (as labeled) melting from the respective sources and melting models.

from a common process or processes, which are probably magmatic. This interpretation, which needs independent tests, is the best choice among several conceivable possibilities (see below).

Bulk-rock REE cannot be explained by melting models but can be explained by post-melting refertilization with caveats

Figure 9 compares site averages (Fig. 7) of bulk-rock REE of abyssal peridotites in primitive-mantle normalized diagrams with simple model melting residues of batch melting (a and c) and fractional melting (b and d) of both an undepleted mantle source such as primitive mantle (a and b) and a depleted mantle (c and d). Clearly, both the abundance levels and patterns are inconsistent with their being simple melting residues. The slopes of the MREE–HREE are better explained by melting regardless of the fertility of the source, and the extent and models of melting. The slopes and patterns of the LREE cannot be explained by either melting model of any fertile source composition. If one chose to believe such modeling to be valid, then batch melting would explain the data better than fractional melting. This is again inconsistent with model conclusions based on residual cpx REE data (Johnson *et al.*, 1990). Prinzhofer & Allègre (1985) suggested that U-shaped REE patterns or LREE enrichments in harzburgites could be modeled by complex partial melting of plagioclase lherzolites. Although the latter modeling may be mathematically useful, such melting is physically unlikely. This is because the plagioclase-lherzolite depth range is equivalent to the TBL beneath ocean ridges, where no melting takes place. Elsewhere, this depth range is within the lithosphere, in which significant melting should not occur anyway. A simple conclusion is that bulk-rock REE in abyssal peridotites

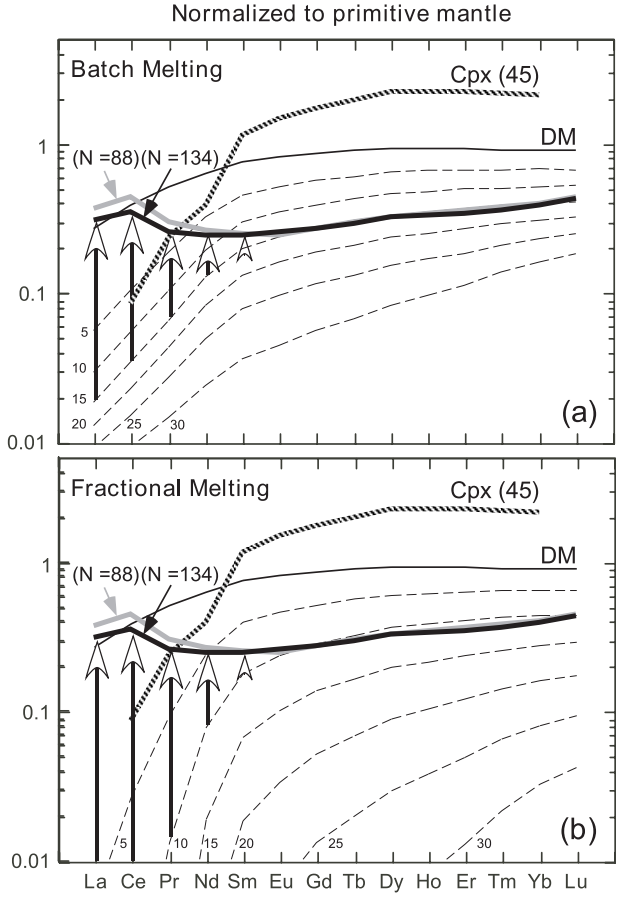

Fig. 10. Same as panels (c) and (d) of Fig. 9, but showing the grand average of sample suites with residual cpx previously studied ($N = 88$; Figs 7 and 9) and the global average of the entire dataset ($N = 134$; Electronic Appendix 1). The MREE and HREE of the averages can be modeled by ~15% batch melting (a) or ~10% fractional melting (b) from a depleted source (Niu & Hékinian, 1997*b*). The elevated LREE can be modeled successfully by adding a less depleted melt component as indicated by the vertical arrows [see Niu & Hékinian (1997*b*) for model details]. However, such refertilization models, despite being effective, are arbitrary in choosing the right amount of the melt with the right compositions for the actual observations (Fig. 9).

cannot be readily explained by melting models of any sophistication at any conceivable depths. Batch melting models better explain REE heavier than Sm, whereas combined batch and fractional melting models can be worse. Melting models face more problems to explain the significant LREE–HFSE correlations (Fig. 8). It is entirely possible that the residual cpx REE data may indeed record melting processes (Johnson *et al.*, 1990). If so, the bulk-rock data must record something else (see below).

If one accepts the significant correlations of LREE with HFSE (Fig. 8) as resulting from magmatic processes, then the elevated LREE abundances in bulk-rock abyssal peridotites can be readily explained by post-melting melt refertilization in the TBL (Fig. 1) as quantitatively evaluated for sample suites from the Garrett Transform [see Niu & Hékinian (1997*b*, fig. 7)]. The modeling can be readily done, but the choice of parameters becomes arbitrary because we need different refertilizing melt compositions and different degrees of enrichments to fit the individual data suites to our satisfaction. The point here is that post-melting refertilization as a hypothesis is the best choice among several conceivable possibilities to explain the bulk-rock REE data. Readers are referred to Niu & Hékinian (1997*b*) for details. Figure 10 illustrates the model schematically for the global average of bulk-rock REE compositions. Figure 10 also shows that the global average ($N = 134$) is very similar to the average ($N = 88$) of samples from Indian ocean ridge–transforms in which residual cpx REE were studied (Johnson *et al.*, 1990; Johnson & Dick, 1992). The MREE–HREE would be consistent with ~10% fractional melting for global MORB genesis (Langmuir *et al.*, 1992), or with ~15% batch melting. The latter mean value of ~15% melting was argued to be consistent with average MORB compositions (Niu & Batiza, 1991) and with primary mineral modes and reconstructed bulk-rock compositions of abyssal peridotites (Niu, 1997; Niu & Hékinian, 1997*b*).

If post-melting refertilization can indeed explain the elevated abundances of LREE in bulk-rock abyssal peridotites, we must then question why such melt refertilization does not seem to have affected the residual cpx (see Fig. 7 and below).

Correlations of REE with MgO

Figure 2 suggests that to a first order, the bulk-rock MgO values still retain some magmatic signals such as the extent of melting or melt depletion. This is supported by examining the correlations between REE and MgO. As REE are incompatible in all residual phases (olivine, opx, cpx and spinel) during partial melting in the spinel peridotite stability field (relevant to the bulk of MORB genesis; see the inverse Sc–MgO correlation above), inverse correlations of REE with MgO are expected. Figure 11 shows representative bulk-rock REE (La, Sm, Dy and Lu) variations against MgO (top four panels). Despite the scattering, the correlation coefficients become progressively more significant from LREE to HREE with the exception of Eu (bottom panel). This is an important observation. To a first order, this suggests that HREE as well as MgO faithfully record the extent of melting or melt depletion even though ~10 wt % relative MgO of the protoliths may have been lost, mostly during seafloor weathering (see below). Because bulk-rock MgO is proportional to modal olivine/(opx + cpx) ratios, and because bulk-rock HREE abundances are mostly controlled by the cpx mode in the rock, the more significant HREE–MgO correlations could simply result from modal heterogeneity given the small size of samples studied. However, the ultimate control remains likely to be

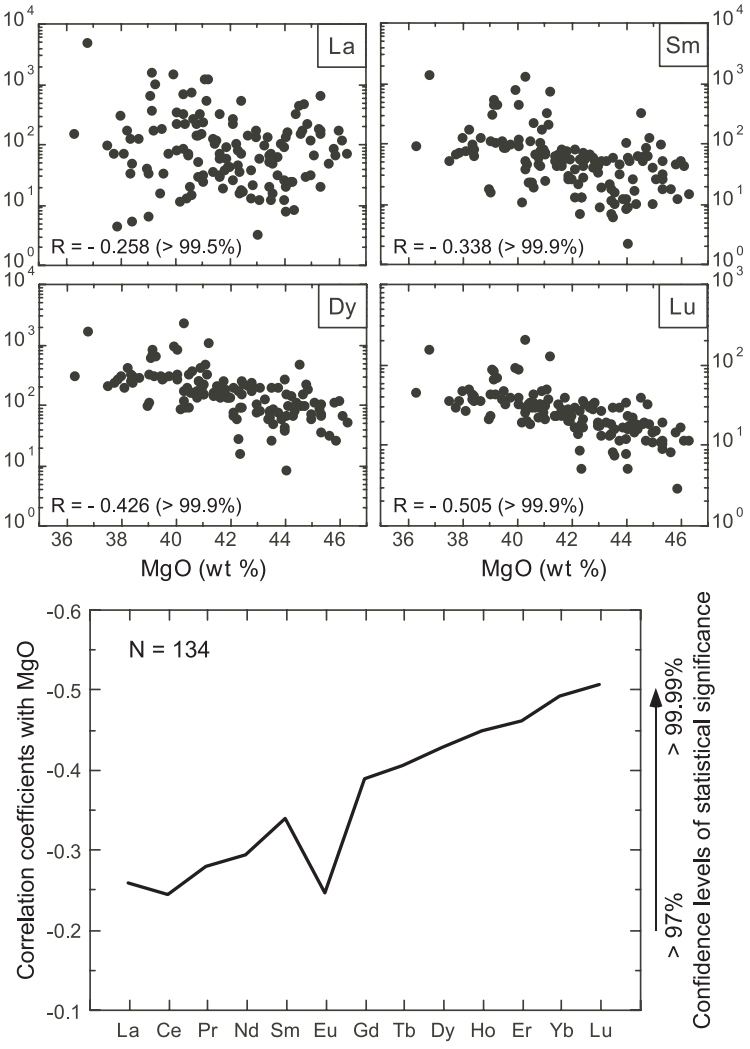

Fig. 11. The scattered yet statistically significant inverse correlations of REE with MgO are consistent with REE being incompatible during mantle melting and with the reasoning that MgO, despite its loss, still retains signatures of mantle melting. The better correlation of MgO with progressively heavier REE (except for Eu), suggests that the HREE tell us more faithfully about mantle melting (see Figs 6, 9 and 10) whereas LREE have experienced post-melting enrichments (Figs 7–9). The poor Eu–MgO correlation may be due to the mobility of Eu^{2+} during serpentinization or seafloor weathering.

melting or melt depletion; that is, with increasing extents of melting, opx and cpx modes decrease whereas olivine modes increase (Fig. 4). Associated with such changes are progressively more depleted mineral compositions—higher Mg-number [Mg/(Mg + Fe)] in olivine, opx and cpx, lower Al_2O_3 in opx and cpx, higher Cr-number [Cr/(Cr + Al)] in spinel (Dick *et al.*, 1984; Niu & Hékinian, 1997*a*; Niu *et al.*, 2003), and reduced REE contents in cpx (also opx) and thus in the bulk-rock samples.

It now becomes clear from Figs 9 and 10 that HREE are indeed consistent with melting or melt depletion as reflected by their better correlation coefficients with bulk-rock MgO. It is also clear that the poor correlations of LREE with MgO result from a post-melting refertilization process, which is arguably magmatic because of significant LREE–HFSE correlations (Fig. 8). In this context, it is noteworthy that the use of coupled major (Cr-number in spinel) and trace element (HREE such as Yb in residual cpx) compositions as indicators of the extent of melting in mid-ocean-ridge peridotites, proposed by Hellebrand *et al.* (2001), are a confirmation of what we have learnt over the last ~30 years (Mysen & Boettcher, 1975; Jaques & Green, 1980; Dick *et al.*, 1984; Falloon & Green, 1988; Niu & Hékinian, 1997*a*). It should be noted also that the extent of melting or melt depletion so calculated may not necessarily reflect the recent sub-ridge melting, but could be inherited from

the fertile mantle source of MORB, which may have experienced previous melt depletion events. Therefore, melting parameters derived from MORB melts (e.g. Niu & Batiza, 1991; Kinzler & Grove, 1992; Langmuir *et al.*, 1992) and abyssal peridotites (e.g. Johnson *et al.*, 1990; Niu, 1997; Hellebrand *et al.*, 2001) must be used with caution when interpreting present-day ocean ridge processes (see below).

Large and correlated variations in both abundances and ratios of HFSE

For many years have we accepted that two elements with the same charge and the same or similar ionic size should behave the same in geological processes. The type examples are the Zr–Hf and Nb–Ta elemental pairs. As a result, there is wide acceptance that Zr/Hf and Nb/Ta ratios should be similar or identical to chondritic values in all terrestrial rocks: Zr/Hf $\sim$ 36·30 and Nb/Ta $\sim$ 17·57 (e.g. Bougault *et al.*, 1979; Hofmann *et al.*, 1986; Jochum *et al.*, 1986; Sun & McDonough, 1989). Although it has been noted that the Zr/Hf ratio varies in carbonatites, and is super-chondritic in some alkali basalts, Niu & Batiza (1997) showed for the first time that these two ratios do vary significantly in lavas from seamounts near the axis of the East Pacific Rise (seafloor basalts) with Zr/Hf $\sim$ 25–50 and Nb/Ta $\sim$ 9–18, respectively. These two ratios are correlated with each other ($R_{Zr/Hf–Nb/Ta} =$ 0·75, statistically significant at >99·9% confidence levels for $N > 80$ samples), and with commonly used index ratios such as Th/U, Nb/U, Rb/Cs, La/Sm, Ce/Yb and Ce/Pb (Hofmann *et al.*, 1986; Hofmann, 1988, 1997; Sun & McDonough, 1989) as well as the abundances of progressively more incompatible elements. All these observations suggest $D_{Zr} < D_{Hf}$ and $D_{Nb} < D_{Ta}$, and also $D_{Nb} < D_{U}$, $D_{Ce} < D_{Pb}$, $D_{Rb} < D_{Cs}$, etc., which disagrees with what is generally accepted. For example, $D_{Cs} < D_{Rb}$ is expected both theoretically and experimentally (Blundy & Wood, 1994), but $D_{Rb} < D_{Cs}$ is observed instead (Niu & Batiza, 1997; Niu *et al.*, 2002*a*). Recent studies of various terrestrial rocks (e.g. Elliott *et al.*, 1997; Godard *et al.*, 2000; Rudnick *et al.*, 2000; Takazawa *et al.*, 2000; Weyer *et al.*, 2002, 2003) and experimental studies have confirmed $D_{Zr} < D_{Hf}$ and $D_{Nb} < D_{Ta}$ (Foley *et al.*, 1999; Green *et al.*, 2000; Tiepolo *et al.*, 2000), but observed no Zr/Hf–Nb/Ta correlations. The recognition of subchondritic Nb/Ta ratios in some terrestrial rocks (e.g. continental crust) has led to speculation of a hidden Nb-rich reservoir deep in the mantle (e.g. McDonough, 1991; Blichert-Toft & Albarède, 1997; Rudnick *et al.*, 2000; Albarède & van der Hilst, 2002; Niu & O'Hara, 2003). Recently, Wade & Wood (2001) suggested that Nb is slightly more siderophile (than Ta) and that a significant amount of the Earth's Nb may be in the core, which may have led to subchondritic Nb/Ta ratios in silicate portion of the Earth. The latter interpretation is supported by super-chondritic Nb/Ta ratios in iron meteorites (e.g. Jochum *et al.*, 2002; Munker *et al.*, 2003). Using the experimentally determined high D_{Nb}/D_{Ta} between amphiboles and hydrous silicate melts (Foley *et al.*, 1999; Tiepolo *et al.*, 2000), Foley *et al.* (2002) proposed that formation and growth of the continental crust might have resulted from partial melting of amphibolites in Earth's early history. All these point to the importance of understanding Nb–Ta fractionation for improved models of chemical differentiation of the Earth and perhaps even aspects of the Solar System.

A factor of two variation of Zr/Hf $\sim$ 25–50 and Nb/Ta $\sim$ 9–18 in seafloor basalts (Niu & Batiza, 1997) can be readily explained by a factor of two bulk distribution coefficient differences (e.g. $D_{Zr}/D_{Hf} \sim 0{\cdot}5$ and $D_{Nb}/D_{Ta} \sim 0{\cdot}5$) (e.g. Green *et al.*, 2000) in terms of melting of a uniform source. However, the statistically significant correlations of Zr/Hf and Nb/Ta with each other and with ratios of other incompatible elements (e.g. La/Sm, Rb/Cs, Th/U, Nb/U, Sm/Yb) as well as radiogenic isotopes (e.g. $^{87}Sr/^{86}Sr$, $^{143}Nd/^{144}Nd$) suggest that the observed Nb–Ta and Zr–Hf fractionations in seafloor basalts (1) do not necessarily reflect recent mantle melting events, but are inherited from their sources with a long history in excess of 1 Gyr (Niu *et al.*, 1999, 2002*a*), and (2) cannot be explained by the slightly siderophile nature of Nb (vs Ta) (Wade & Wood, 2001) because the Earth's core would not, for example, preferentially take Zr (vs Hf), La (vs Sm), Rb (vs Sr), Nd (vs Sm), etc. Therefore, there must be another process or processes that cause the observed Nb–Ta and Zr–Hf fractionations in seafloor basalts (Niu & Batiza, 1997). Significant Nb/Ta variations in arc lavas (e.g. Elliot *et al.*, 1997) could be due to the subducting slab melting with rutile as a residual phase (Klemme *et al.*, 2002), which may in turn help explain Nb/Ta fractionations in oceanic basalts as a result of crustal recycling. However, such a process cannot explain the correlated variations of Nb/Ta and Zr/Hf in seafloor basalts (Niu & Batiza, 1997) and abyssal peridotites (see below).

Figure 12 shows the variation of Nb/Ta vs Zr/Hf for $\sim$130 bulk-rock abyssal peridotite samples (Electronic Appendix 1). The statistically significant Nb/Ta vs Zr/Hf correlation, and the over two orders of magnitude variations of the two ratios well exceed the data range defined by seafloor basalts ($N > 80$, open squares within the ellipse) (Niu & Batiza, 1997). Analytical uncertainties and the small size of samples studied may cause the apparent scatter, but both the trend and much of the scatter are probably a consequence of physical processes that need to be understood. In other words, improved analytical precision will not significantly reduce the scatter because the scatter is probably part of the random 'sampling' processes beneath ocean ridges: where, how,

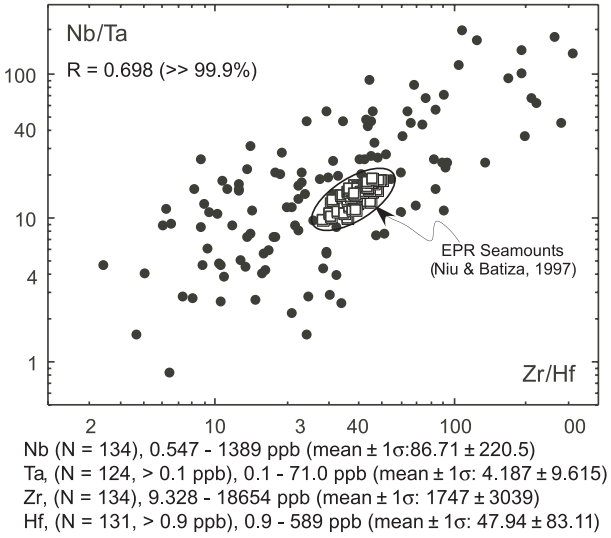

Fig. 12. Scattered, yet statistically significant ($R = 0{\cdot}698$ for $N = 131$), correlation between Zr/Hf and Nb/Ta ratios of abyssal peridotites and near East Pacific Rise (EPR) seamounts (open squares). The chondritic ratios of Nb/Ta = 17·57 and Zr/Hf = 36·30 (Sun & McDonough, 1989) lie within the ellipse defined by the EPR seamount data.

to what extent and the nature of the interactions between ascending melts and advanced residues, as well as the likely scenario that the composition and the amount of trapped melt vary in space and time (see Fig. 1 and discussion below). Figure 13 compares the variation of Nb, Ta, Zr and Hf vs Ce and $[Sm/Yb]_N$ within the bulk-rock data. The significant positive trends suggest that data for the analytically 'difficult' elements such as Ta (and Nb) and Hf (and Zr) vs analytically easy elements such as Ce, Sm and Yb are of good quality (also see Electronic Appendix 1 for analytical precisions). Figure 13 also suggests that the data trends are magmatic (vs serpentinization). Figure 14 illustrates Nb/Ta and Zr/Hf ratios against Ce, Be/Tb, Ce/Y, and La/Yb (LREE/HREE) for the bulk-rock data. Although scattered, the significant positive trends again are best explained by magmatic processes.

How mobile are incompatible elements during serpentinization and seafloor weathering?

Any element can be mobile during hydrothermal metamorphism, such as serpentinization, if no stable minerals exist that can host that particular element and if the element is soluble in the fluid being transported (Niu & Lesher, 1991). If an element is mobile during serpentinization, either added or removed or relocated on some scales, the behavior of this element should be decoupled from that of more immobile elements. For example, both Th and U are similarly incompatible during magmatic processes: these two elements whether depleted or enriched should correlate very well with each other, as is often observed. On the other hand, if Th behaves as an immobile element whereas U is mobile during serpentinization or seafloor weathering, these two elements will be decoupled from each other and there will be no correlation between the two elements in these peridotites. On the other hand, if two elements are both immobile, their correlation may not necessarily be good if they have very different incompatibility during magmatic processes. For example, $R_{Nb–Ti}$ is unlikely to be as good as $R_{Nb–Ta}$. We can use these criteria to see how mobile incompatible elements of interest may be during serpentinization or seafloor weathering.

Figure 15 demonstrates the correlation coefficients between the 'immobile' incompatible elements Ti, Zr, Nb and Th and all other incompatible elements. The correlation coefficients are sorted in decreasing order from left to right. For $N > 130$, $R > 0{\cdot}3$ is statistically significant at >99·9% confidence levels. We thus arbitrarily consider $R > 0{\cdot}3$ to be more meaningful correlations. For each of the above elements, their correlation coefficients with other elements are best with elements of similar incompatibility. For example, Ti correlates better with HREE, Zr with MREE and some LREE, Nb with LREE, Ba, Ta, and Th with LREE, Nb, Ta, etc. If we consider all these correlation coefficients, we find that the incompatible elements Rb, Cs, U, Sr and Na do not correlate in more significant ways with all the other elements in Fig. 15. As expected, these are indeed elements readily mobilized in aqueous solutions such as during serpentinization or perhaps as a result of seafloor weathering. For all other elements, because their correlations are consistent with their relative incompatibilities (i.e. magmatic behaviors), they are largely immobile during serpentinization or seafloor weathering. Some aspects of this behavior have been demonstrated by the significant correlations between LREE and HFSE (Fig. 8) and between REE and MgO (Fig. 11). Although some of these correlations are not unexpected, the emphasis is necessary for a better understanding of sub-ridge mantle processes.

It is somewhat surprising, however, that Ba and Pb, which are often considered to be highly mobile during hydrothermal alteration such as massive sulfide mineralization (Niu & Lesher, 1991) and subduction-zone dehydration processes (see Niu & O'Hara, 2003, table 1), do not seem to be mobile during serpentinization (or seafloor weathering). Instead, these two elements in bulk-rock abyssal peridotites exhibit geochemical behaviors consistent with their being highly incompatible elements (Fig. 16). What is more surprising is that Pb seems to be as incompatible as, or more so than, Th, Nb, La and Ce. Such a highly incompatible behavior of Pb is consistent with K_d values obtained experimentally (Hauri *et al.*, 1994), but more incompatible than inferred from oceanic

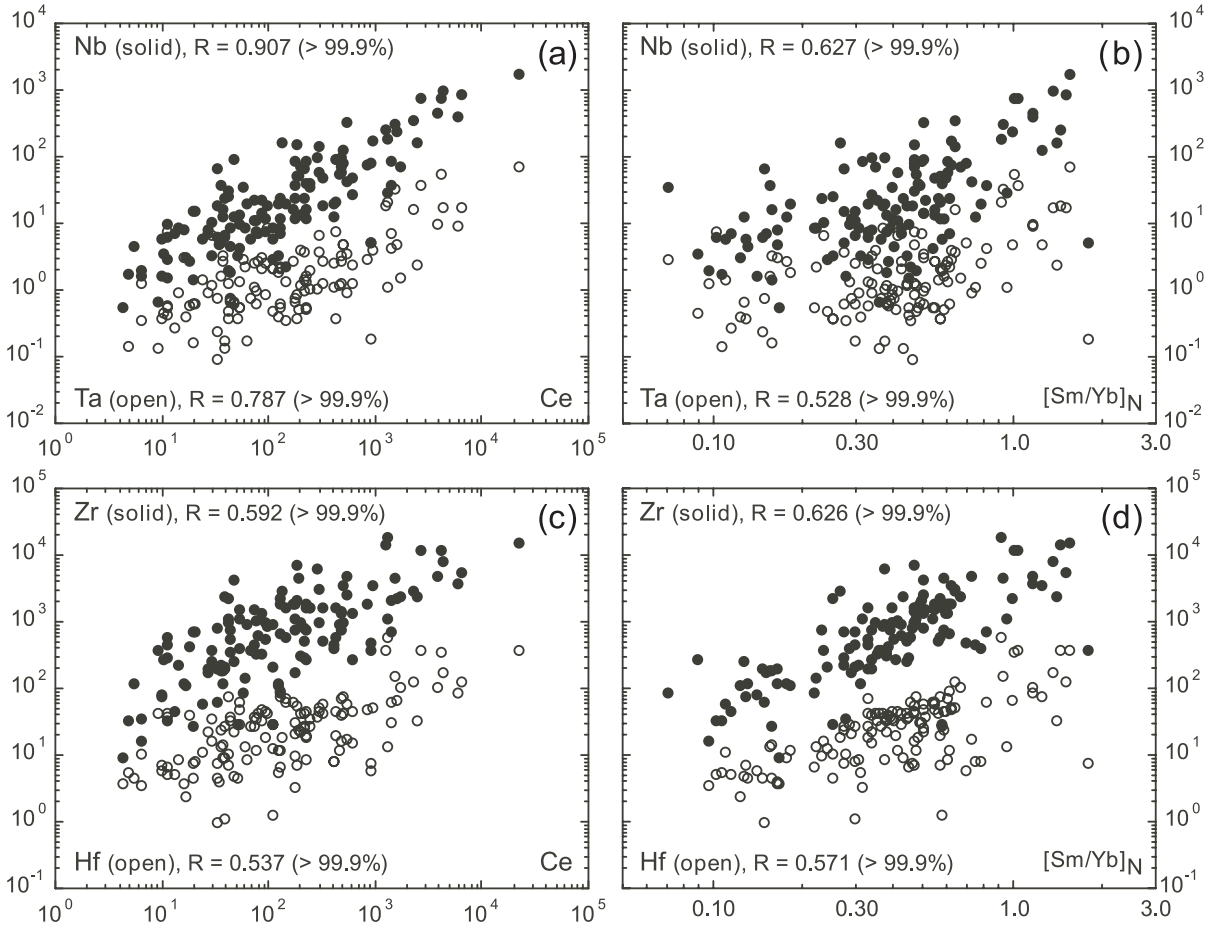

Fig. 13. The scattered yet statistically significant correlations of Nb, Ta, Zr and Hf with Ce and $[Sm/Yb]_N$ indicate that these analytically 'difficult' HFSE and analytically 'easy' REE both are of good quality (also see Electronic Appendix 1 for details). Such correlations are best explained by magmatic processes.

basalts (e.g. Hofmann *et al.*, 1986; Sun & McDonough, 1989; Niu & Batiza, 1997). The variable and overall higher abundances than in average MORB suggest that Pb in bulk-rock abyssal peridotites, together with many other highly incompatible elements (Figs 6–10), may come from melt refertilization (see below).

DISCUSSION

Where does the refertilization occur?

Figure 1 shows that mantle decompression melting stops at a level deep within the mantle (P_f) because of conductive cooling to the surface (Niu, 1997), which defines the base of the 'cold' thermal boundary layer (TBL) (Niu *et al.*, 1997), whose thickness increases with decreasing plate separation rate (Niu & Hékinian, 1997*a*). Decompression melting may stop as deep as >30 km beneath very slow-spreading ridges (Niu, 1997). The TBL comprises advanced residues of previous melting at depth. Although no melting occurs within this 'cold' TBL, the ascending new melts will pass through and interact with the advanced residues on their way to the crust. Hence, the TBL is the logical place for post-melting refertilization or melt–solid interactions. It should be noted that dunite dikes or veins as seen in mantle sections of ophiolites (e.g. Kelemen *et al.*, 1995, 1997; Braun & Kelemen, 2002) may well develop in this TBL. However, abyssal peridotites (harzburgitic and/or lherzolitic) are arguably residual materials sampled away from these possible or probable dunite bodies. It is also noteworthy that serpentinization is a late and shallow level (constrained by some maximum depth of seawater penetration) process relative to melt refertilization (or melt–solid interactions) in the TBL for all the abyssal peridotite samples so far collected and studied.

In this context, we should emphasize that partial melting in the plagioclase-peridotite stability field may not occur at all in practice despite its theoretical significance (Prinzhofer & Allègre, 1985; Asimow *et al.*, 1995; Yang

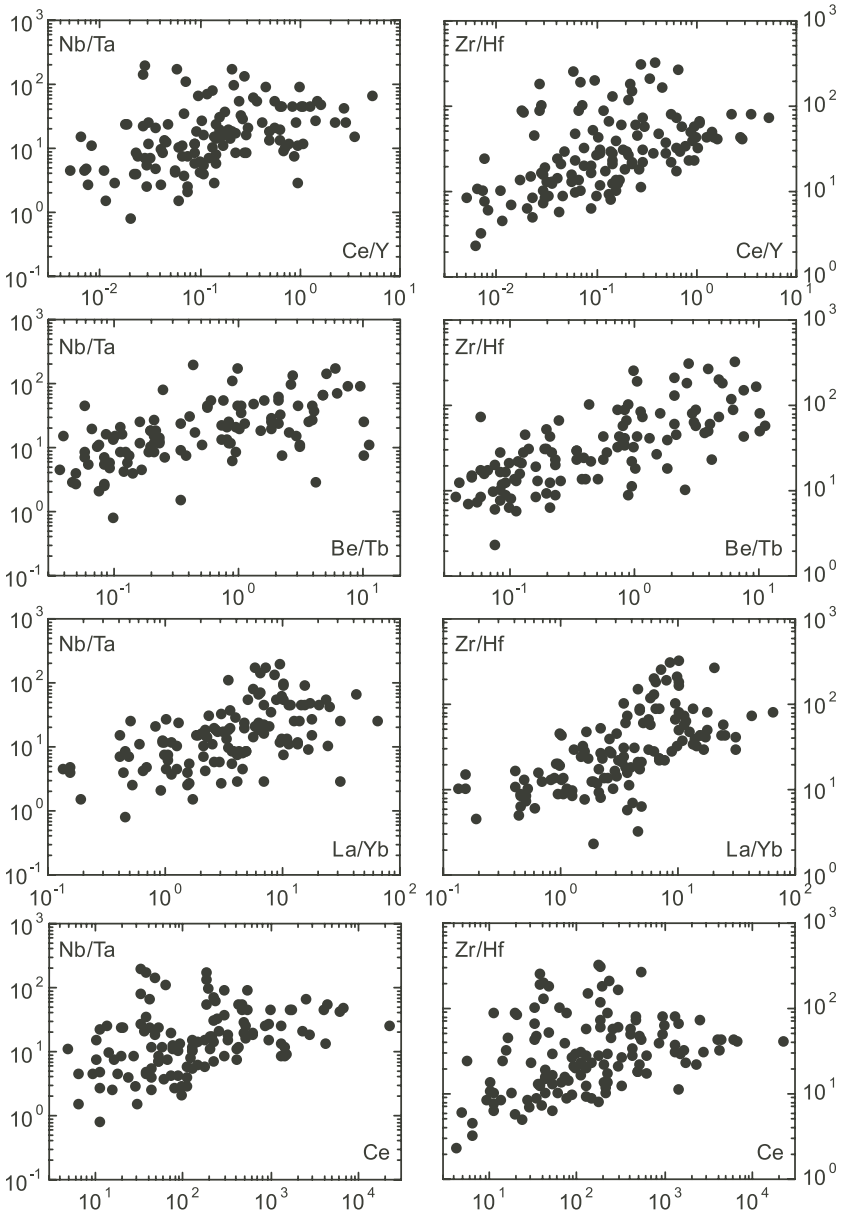

Fig. 14. The scattered yet correlated trends of Nb/Ta and Zr/Hf with Ce and ratios of more incompatible elements over less incompatible elements (Ce vs Y, Be vs Tb, La vs Yb) are not only consistent with the notion that Zr is more incompatible than Hf and Nb is more incompatible than Ta, but also suggest that Nb–Ta and Zr–Hf fractionations are caused by magmatic processes.

et al., 1998). Beneath mid-ocean ridges, the plagioclase peridotite stability range is equivalent to the 'cold' TBL, where no melting takes place, particularly beneath slow-spreading ridges (including continental rift systems). Elsewhere, this depth range is within the lithosphere, which, by the definition of plate tectonics, is too cold to melt. Hence, the concept that sub-ridge mantle decompression melting continues all the way to the base of the crust (Klein & Langmuir, 1987; McKenzie & Bickle, 1988) should be abandoned in evaluating the extent and depth of melting (Niu, 1997). However, in the context of mantle plume–lithosphere interactions, the lithospheric mantle (spinel- and plagioclase-peridotites) may participate in the melting processes as a result of 'thermal erosion' or assimilation if the heat from the plume is adequate (O'Hara, 1998).

Why does such melt refertilization seem not to have affected the residual cpx?

If the refertilization is magmatic, why does this process not affect cpx? There are two possibilities. (1) It is too

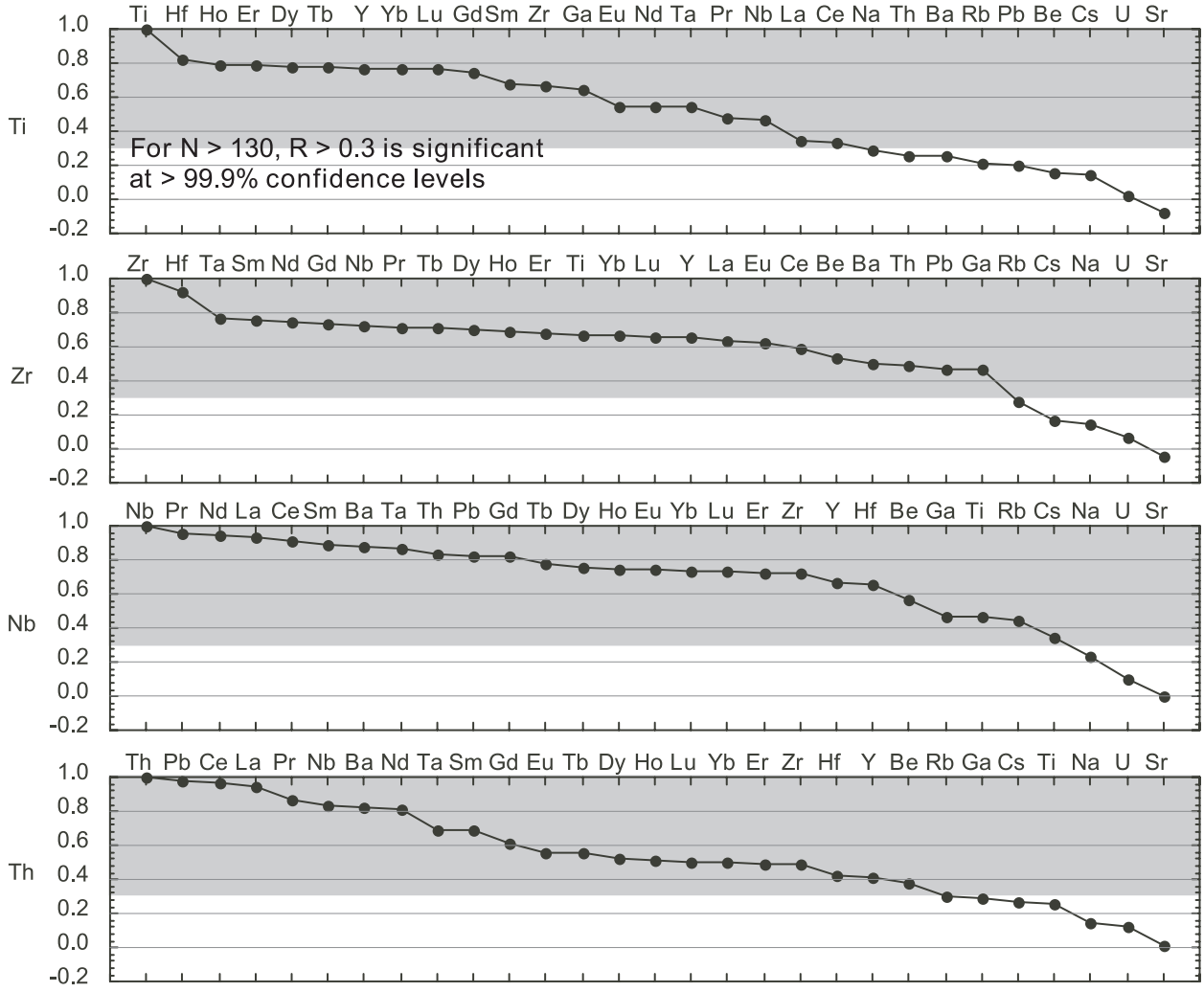

Fig. 15. Plots of correlation coefficients of the relatively immobile incompatible elements Ti, Zr, Nb and Th with all other incompatible elements. The significant correlations ($R > 0{\cdot}3$) would suggest that the elements of interest are immobile during serpentinization or seafloor weathering. The degrees of correlation also depend on similarity of incompatibility, i.e. similarity in magmatic behavior. For example, $R_{Zr–Hf}$ is significantly better than $R_{Zr–Ti}$ and $R_{Zr–Nb}$.

'cold' in the TBL so that the ascending melt is unable to react with cpx, but cools and crystallizes out whatever minerals are on the liquidus, in this case olivine plus Cr-spinel, with some melt trapped along grain boundaries, giving rise to excess olivine (Niu *et al.*, 1997; Niu, 2003, submitted) and elevated abundances of LREE, HFSE and other incompatible elements in the bulk-rock samples. (2) Alternatively, melts ascending and percolating through the TBL affect only 'rims' of cpx. These affected rims are later serpentinized together with the rest of the rock. The analyzed portions of cpx are only 'cores' that were unaffected by the ascending melts and also survived subsequent serpentinization. Let us suppose the advanced melting residues with some cpx grains in the TBL are similar to those in Fig. 17a. The ascending melts will migrate and percolate through the residues along grain boundaries and cracks as in Fig. 17b. Subsequent serpentinization at a much shallower level (Fig. 1) will preferentially start and extend from grain boundaries and cracks as in Fig. 17c. As a result, the rims of the cpx grains that were affected by magmatic reaction or refertilization will become serpentinized, whereas the analyzed cpx relics or 'cores' (e.g. Johnson *et al.*, 1990), which were unaffected by the refertilization in the first place, remain unaltered. In either of the two scenarios, the following reasoning should be valid.

(1) Melts ascending through the advanced residues in the TBL beneath mid-ocean ridges will interact with the residues on scales smaller than hand-specimen (or thin-section) size.

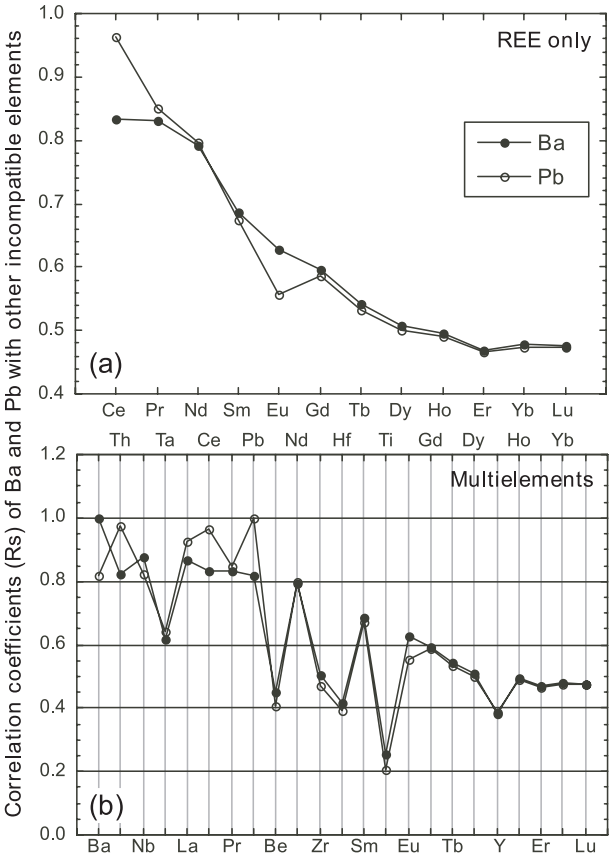

Fig. 16. Correlation coefficients of Ba and Pb with REE (a) and other incompatible elements (b). The significant correlations of Ba and Pb with LREE, Th, Nb, etc. suggest that Ba and Pb are not mobile during serpentinization or seafloor weathering.

(2) The melt is not necessarily chemically reactive with the solid residues (at least in terms of LREE and HFSE).

(3) Porous flow along grain boundaries (perhaps also crystal cracks) is significant even at depths as shallow as the TBL beneath mid-ocean ridges. It should be noted that although dunite bodies representing probable melt channels may exist in the TBL, and may be significant in terms of melt transport, abyssal peridotites record porous melt flows on much finer scales.

Storage and distribution of excess LREE, HFSE and other incompatible elements

The above reasoning leads to the conclusion that 'excess' incompatible elements in abyssal peridotites must physically reside in serpentine or highly serpentinized domains. It is necessary to know the way in which these elements are distributed within the rock because this information tells us the nature of possible 'melt–solid' interactions during melt migration through advanced residues to the crust. 'Smoking-gun' evidence for the exact storage and distribution of the excess incompatible elements requires elemental mapping with advanced techniques such as laser-ablation ICP-MS, aided by careful petrography and SEM. Several possible scenarios are worth considering.

(1) If the 'excess' incompatible elements concentrate as trails marking primary (prior to serpentinization) grain boundaries, this would suggest a rather passive 'melt–solid' interaction, similar to 'cryptic metasomatism' seen in the subcontinental lithosphere (e.g. O'Reilly & Griffin, 1988; Bodinier *et al.*, 1996). This would occur if the melt is under cooling and fails to react chemically with the minerals in the advanced residues, but crystallizes liquidus minerals (e.g. olivine plus Cr-rich spinel) with traces of melt left behind (trapped) on its path of migration (e.g. Niu & Hékinian, 1997*b*; Niu *et al.*, 1997).

(2) If the abundances of these 'excess' elements show spatial gradients or patterns with respect to primary grain boundaries or certain residual phases such as cpx and opx, this would favor the interpretation of 'significant melt–solid interaction'. For example, olivine may precipitate while both cpx and opx dissolve into the melt (e.g. Kelemen *et al.*, 1995, 1997; Niu, 1997; Lundstrom, 2000). This would require a hot melt with probably super-liquidus temperatures. Such melt–solid interaction or reaction, in the form of $\mathrm{Melt_A} + \mathrm{Cpx} + \mathrm{Opx} \Rightarrow \mathrm{Ol} + \mathrm{Melt_B}$ with mass ratios $M_{\mathrm{MeltB}}/M_{\mathrm{MeltA}} > 1$ (e.g. Niu & Batiza, 1993; Kelemen *et al.*, 1997), is in essence the same as the isobaric incongruent equilibrium melting reaction (Kinzler & Grove, 1992; Baker & Stolper, 1994) or decompression melting relationship in the spinel peridotite stability field (Niu, 1997, 1999): a Cpx + b Opx + c Spinel $\Rightarrow$ d Ol + 1·0 Melt (also see Fig. 4). The latter occurs in the decompression melting region and will not take place in the TBL, which is, by definition, 'too cold for melting to occur' (see Fig. 1). Also, among all the major phases in the TBL (olivine, opx, cpx and spinel), cpx (and to lesser extent opx) is by far most important in hosting LREE and other incompatible elements (e.g. Frey, 1969; Nagasawa *et al.*, 1969; Shimizu, 1975; Eggins *et al.*, 1998). It follows that dissolution of cpx (also opx) will enrich incompatible elements in the resultant $\mathrm{Melt_B}$ (note—there is a 'counter' dilution effect as melting proceeds) by depleting the bulk solid residues. This is, however, inconsistent with the observation that bulk-rock abyssal peridotites are enriched, not depleted, in LREE and other incompatible elements (Figs 6–10). Incomplete melt extraction (i.e. the presence of trapped melt) will satisfy the observation of excess incompatible elements in bulk-rock compositions. However, such reaction or reactions will not create excess olivine in abyssal peridotites (Niu *et al.*, 1997; Niu, 2003) because the amount of olivine

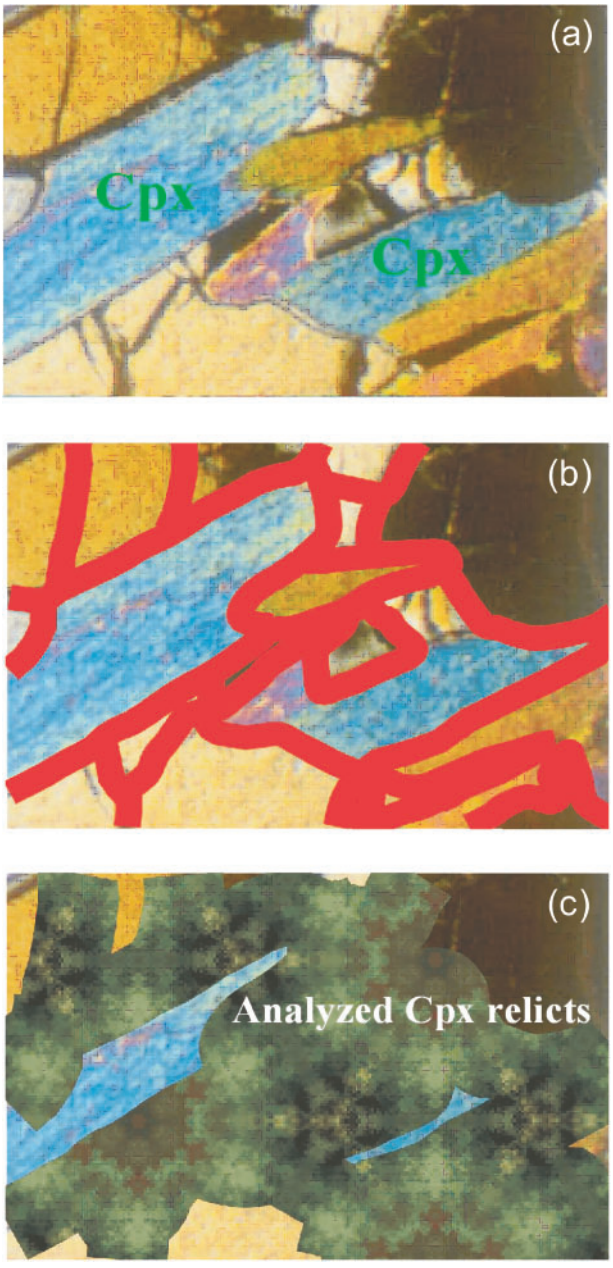

Fig. 17. A conceptual illustration that post-melting magmatic refertilization affects only rims, not 'cores', of residual cpx. The rims are subsequently serpentinized. The analyzed 'cores', which survived serpentinization, thus show no effect of post-melting refertilization. (a) Fresh peridotite in the thermal boundary layer (Fig. 1). (b) Melt percolating along grain boundaries and cracks. (c) Serpentinization extends from grain boundaries and cracks; only cpx relicts are analyzed, thus showing no evidence for melt refertilization.

produced is constrained by the incongruent melting reaction and no excess olivine can be created without cooling (Niu, 2003, submitted). Obviously, this scenario has conceptual problems and is also inconsistent with observations.

(3) Alternatively, the 'excess' incompatible elements may be distributed randomly in serpentines or highly serpentinized domains of bulk-rock abyssal peridotites. This scenario, if true, cannot be readily explained in terms of physically understood processes. One likely possibility is the presence of some 'exotic' phases, which may account for much of the excess LREE, HFSE and possibly other incompatible elements. Such 'exotic' phases could be primary or ancient, and might also have survived recent sub-ridge mantle melting. For example, Brandon *et al.* (2000) argued that the apparent Pt–Os isotope paradox in abyssal peridotites (MARK suite from the Atlantic) is best explained by ancient melting (vs recent MORB genesis) with residual sulfides or metal alloys (probably Pt–Os hosts) isolated from recent melting events. The excess LREE and HFSE in abyssal peridotites are not expected to be stored in sulfides, but we cannot rule out the possible presence of other 'exotic' phases. Alternatively, the 'exotic' phases may be produced during decompression melting or melt–solid interactions in the TBL although how they could form is unknown. Whether the possible or probable 'exotic' phases were ancient or produced in recent sub-ridge processes, their presence in bulk-rock abyssal peridotites, if there are any at all, may have huge 'nugget effects' (e.g. Wang *et al.*, 1999; O'Hara *et al.*, 2001*a*, 2001*b*), which may help explain the very large abundance variations of Nb, Ta, Zr and Hf, and perhaps also highly fractionated Nb/Ta and Zr/Hf ratios (see below). The hypothesis for the presence of 'exotic' phases is favored by the observation that excellent analytical reproducibility is readily achieved from the same digested or dissolved solutions (complete digestion is ensured using 'bombs'), but not so from different digestions or dissolutions of the same sample even though the samples are carefully ground (in an agate mill in an ultraclean environment) and homogenized to extremely fine size; the 'exotic' phases, which are probably volumetrically small, do not distribute uniformly.

What causes Nb–Ta and Zr–Hf fractionation?

If we accept that $D_{Zr}/D_{Hf} < 1$ and $D_{Nb}/D_{Ta} < 1$, it becomes straightforward why Nb–Ta and Zr–Hf fractionations take place in magmatic processes. However, we do not really understand in theory why $D_{Zr}/D_{Hf} < 1$ and $D_{Nb}/D_{Ta} < 1$ should be the case. It is also unclear how $D_{Zr}/D_{Hf} \sim 0{\cdot}5$ and $D_{Nb}/D_{Ta} \sim 0{\cdot}5$ can readily explain the huge Nb–Ta and Zr–Hf fractionations seen in abyssal peridotites (Figs 12 and 14).

So far, the 'lattice strain' model (Blundy & Wood, 1994; Wood & Blundy, 1997) is perhaps the most successful

thermodynamic model in predicting partitioning behavior of an element during magmatic processes. This model, however, remains charge and size dependent, as is the use of Onuma plots (Onuma *et al.*, 1968). Given the identical charges (5^+ for Nb and Ta, and 4^+ for Zr and Hf) and essentially the same ionic radii ($R_{Nb}/R_{Ta} = 1{\cdot}000$ and $R_{Zr}/R_{Hf} = 1{\cdot}006$ to $\sim 1{\cdot}026$ for coordination numbers of 6, 7, 8 and 12) of the two elemental pairs (e.g. Klein & Hurlbut, 1999), the lattice strain model does not apply to Zr–Hf and Nb–Ta fractionations. Also, the lattice strain model predicts $D_{Rb} > D_{Cs}$ (Blundy & Wood, 1994), but the observation is $D_{Rb} < D_{Cs}$ (Niu & Batiza, 1997).

Given that the elemental pairs Zr–Hf and Nb–Ta have the same charges and similar ionic radii but a factor of two differences in their respective atomic masses ($M_{Zr}/M_{Hf} = 0{\cdot}511$; $M_{Nb}/M_{Ta} = 0{\cdot}513$), it is logical to reason that mass differences may have effects on the observed fractionations (or the apparent relative incompatibility). For example, for two elements of similar or identical chemical properties the lighter element (e.g. $^{90-92}$Zr, ^{93}Nb) is more incompatible than the heavier element (e.g. $^{177-180}$Hf, ^{181}Ta) (Niu & Batiza, 1997). This allowed Niu & Hékinian (1997*b*) to suggest mass-dependent fractionation, either differential diffusion rates or differential mass transfer rates. Such mass-dependent fractionation may also explain why $D_{Rb} < D_{Cs}$ (mass ratio $M_{Rb}/M_{Cs} = 0{\cdot}643$) even though Cs is about 10% larger in ionic radius than Rb. The $\sim$50% mass difference for Zr–Hf and Nb–Ta is significantly greater than commonly considered isotopic fractionations of light stable elements at relatively low temperatures; however, it is possible that our present knowledge is incomplete and that mass fractionation of heavy metals at high-temperature mantle conditions may be possible. The ultimate test for the hypothesis of mass-dependent fractionation requires well-designed experimental studies and isotopic analyses of 'serpentinization-resistant' (or immobile) elements at different mass levels (e.g. ^{46,47,48,49,50}Ti, ^{90,91,92,94,96}Zr, ^{174,176,177,178,179,180}Hf) in abyssal peridotites using multiple collector ICP-MS. We should recognize, however, that diffusion or mass transfer coefficients are known to be mass dependent. For example, $D_A/D_B = (M_B/M_A)^{1/2}$, where D_A and D_B represent diffusion coefficients of species with mass M_A and M_B, respectively (Peterson, 1974; Lasaga, 1998). For a mass ratio of $\sim$2 (e.g. M_{Ta}/M_{Nb} and M_{Hf}/M_{Zr}), the diffusion coefficient ratio would be D_{Nb}/D_{Ta} (or D_{Zr}/D_{Hf}) = 1·414, i.e. the lighter element would diffuse, under ideal situations, $\sim$41% more efficiently than the heavy element (given all other variables the same: same charge, same ionic radius, same coordination number, etc.). That is, there would be an $\sim$41·4% fractionation just from the mass-dependent diffusion coefficients. Such $\sim$41% (or 410‰) fractionation contrasts with familiar per-mil level light isotope fractionations. For example, for ^{16}O and ^{18}O fractionation, $D^{18O}/D^{16O} = (16/18)^{1/2} = 0{\cdot}943$, there would be a 57‰ fractionation.

Is it possible that the apparent $D_{Zr}/D_{Hf} < 1$, $D_{Nb}/D_{Ta} < 1$ and $D_{Rb}/D_{Cs} < 1$ may be due to mass differences? Can mass fractionation of heavy metals take place under mantle conditions? Or can serpentinization process lead to the huge Zr/Hf and Nb/Ta fractionations in abyssal peridotites (Figs 12–14)?

Nb–Ta and Zr–Hf fractionation beneath mid-ocean ridges—a hypothesis

Earlier it was stressed that the observed Zr–Hf and Nb–Ta fractionation in seafloor basalts (Niu & Batiza, 1997) is not caused by recent sub-ridge mantle melting, but is inherited from a fertile source that has had a long history in excess of 1 Gyr. Supporting evidence is provided by the correlated variations of Zr/Hf and Nb/Ta with other incompatible element ratios (e.g. La/Sm, Sm/Yb, etc.) and radiogenic isotopic ratios (e.g. ^{87}Sr/^{86}Sr, ^{143}Nd/^{144}Nd, etc.) (Niu *et al.*, 2002*a*). It should also be noted that, as widely accepted, MORB-source mantle is heterogeneous with at least two components [see Hirschmann & Stolper (1996) for details]. Volumetrically small dikes or veins (enriched in volatiles and incompatible elements, with radiogenic Sr and unradiogenic Nd, and high Zr/Hf and Nb/Ta ratios, etc.) are dispersed in a more depleted peridotitic matrix (Niu *et al.*, 1999, 2002*a*; Wendt *et al.*, 1999; Salters & Dick, 2002). The enriched component (dikes or veins) must be of low-degree (low-*F*) melting origin because low-*F* melts host the highest abundances of incompatible elements, and because low-*F* melting can effectively fractionate elements with only subtle differences in incompatibility (e.g. Nb vs Ta and Zr vs Hf). The depleted matrix, which provides the major source component of highly depleted seafloor basalts, is also consistent with low-*F* processes. For example, if the enriched lithologies (the product of the low-*F* melts) have only slightly super-chondritic Nb/Ta and Zr/Hf ratios, the residues of the low-*F* melts must be substantially subchondritic (Niu *et al.*, 2002*a*; Niu & O'Hara, 2003). This is an important concept to keep in mind when understanding possible Nb–Ta and Zr–Hf fractionation beneath mid-ocean ridges at present.

We cannot entirely rule out the possibility that the huge Zr–Hf and Nb–Ta fractionations in abyssal peridotites (Figs 12 and 14) may be inherited from fertile mantle sources (including random distribution of some 'exotic' phases and their 'nugget' effects; see above) and survived recent melting events involved in MORB genesis. However, such 'exotic' phases could also be produced as a result of melt–solid interactions in the TBL. All these possibilities need testing by examining the distribution and storage of HFSE and other 'excess' incompatible elements in abyssal peridotites.

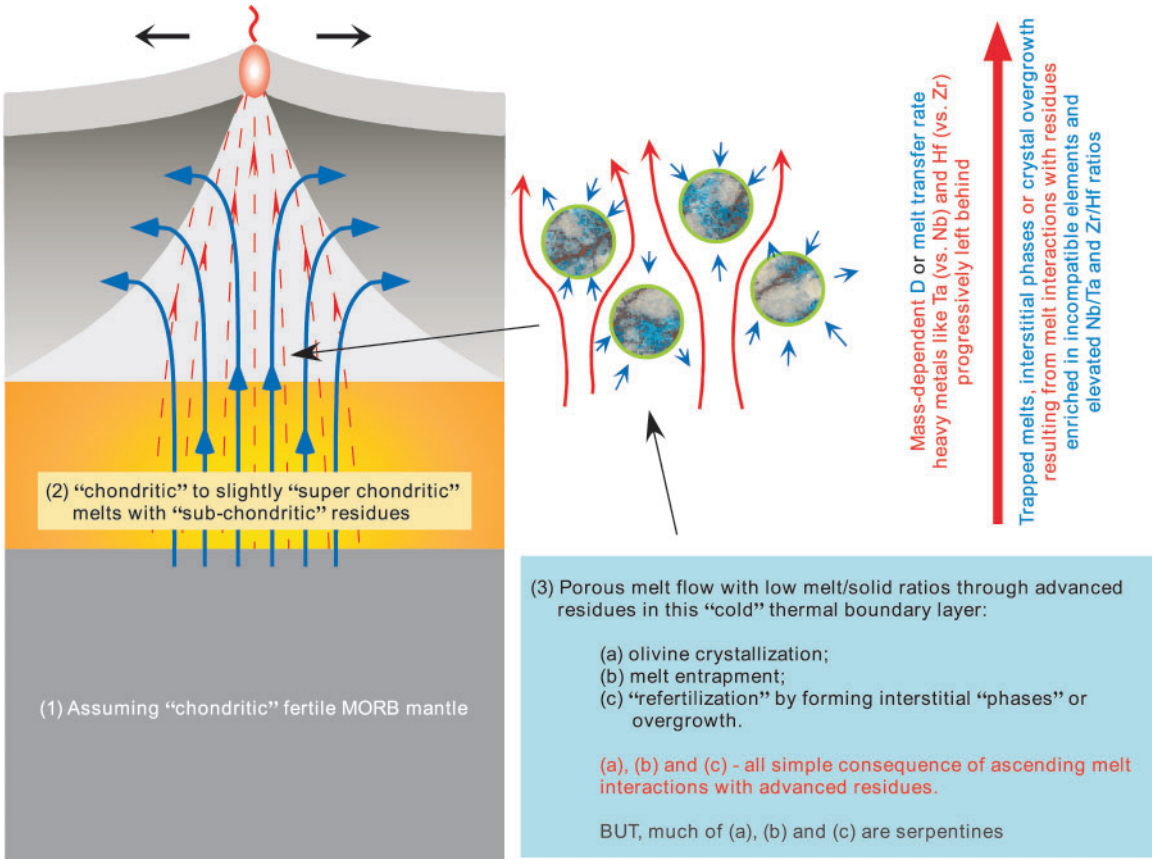

Fig. 18. Illustration of the hypothesis that the large Zr–Hf and Nb–Ta fractionations in abyssal peridotites may have resulted from ascending–percolating melt interaction with the advanced residues in the thermal boundary layer beneath mid-ocean ridges (also see Fig. 1). The process may be very similar to the chromatographic process (Navon & Stolper, 1987), but mass-dependent elemental fractionation may be significant.

Below, I describe a preferred hypothesis that the very large Zr–Hf and Nb–Ta fractionations in abyssal peridotites may have resulted from a conceptually familiar chromatographic process, which is geochemically well understood in the laboratory, but remains rather elusive (e.g. Navon & Stolper, 1987). This hypothesis cannot yet be readily tested through theoretical modeling of any sophistication, but requires additional observations. For example, understanding the storage and distribution of HFSE and all other incompatible elements in serpentinized peridotites will provide clues as to whether such a process is important in nature. This is currently under consideration using LA-ICP-MS techniques. A definite test requires detailed mineralogical and geochemical mapping of exposed mantle sections equivalent to the TBL beneath a paleo-ridge. Figure 18 illustrates the key elements of the hypothesis. (1) Let us suppose, for simplicity, that the fertile MORB-source mantle has chondritic Nb/Ta and Zr/Hf ratios. (2) Partial melts of such a source will have slightly super-chondritic ratios (because of $D_{Nb} < D_{Ta}$ and $D_{Zr} < D_{Hf}$), but the residues will be highly depleted in Nb, Ta, Zr and Hf with substantially subchondritic Nb/Ta and Zr/Hf ratios. (3) The residues will rise passively to the TBL (the triangular grey area). Newly formed melts (dashed red lines with arrows) from below will rise, and percolate along grain boundaries (red lines with arrows) within the advanced residues in the TBL. Because of mass-dependent bulk D or transfer rate (preferred hypothesis; see above), lighter metals such as Nb and Zr will move faster than heavy ones such as Ta and Hf. The heavier metals such as Ta (vs Nb) and Hf (vs Zr) are progressively left behind, leading to localized melts enriched in lighter elements (e.g. high Nb/Ta and Zr/Hf ratios) towards shallower levels in the TBL. This process is likely to take place at conditions of low melt/rock ratios. The 'chromatographic effects' discussed here emphasize mass-dependent differential elemental transfer rates, or mass-dependent bulk D values vs experimentally determined K_d values or bulk D values. This process is probably accompanied by (a) olivine addition, (b) melt entrapment and/or (c) refertilization by forming interstitial 'phases' (exotic?) or crystal overgrowth. All these, taken together, are simple consequence of ascending melt interactions with advanced residues in the TBL. In

this context, we may speculate about the possibility that the elevated LREE abundances in the bulk-rock abyssal peridotite samples could also be produced or perhaps enhanced by mass-dependent element transfer, i.e. lighter REE (vs heavier REE) would transfer faster, leading to advanced residues progressively refertilized with LREE-rich melt towards shallower levels (see Figs 6–10) to be sampled as abyssal peridotites. This possibility awaits observational tests.

Abyssal peridotites sampled from the seafloor probably represent random samples atop the TBL. Individual samples may have experienced different extents of 'melt–solid' interaction. If the sample had experienced little such interaction with a limited amount of trapped melt, this sample would be depleted in incompatible elements with low Nb/Ta and Zr/Hf ratios. Conversely, if the sample had experienced pervasive 'melt–solid' interaction with significant amounts of trapped melt, it would have elevated abundances of incompatible elements and high Nb/Ta and Zr/Hf ratios.

Is cpx a residual phase or an exsolution product?

Abyssal peridotites are apparently metamorphosed and deformed under subsolidus conditions (even prior to serpentinization) (Dick, 1989; Niu, 1997, 1999; Niu & Hékinian, 1997*b*; Niu *et al.*, 1997). It is thus possible that at least some of the cpx grains previously analyzed for trace elements (Johnson *et al.*, 1990) may have exsolved from residual opx by 'granular' exsolution (Lindsley & Anderson, 1983) under subsolidus conditions. Cpx with depleted incompatible element signatures might have inherited these from the precursor opx instead of reflecting melting processes. If this is indeed true, then the interpretation of 'near-perfect fractional melting' based on cpx trace element data needs revision. Cpx lamellae in opx within some less serpentinized abyssal peridotites are common but volumetrically small (Dick *et al.*, 1984; Dick & Natland, 1996; Niu & Hékinian, 1997*b*). It is possible that in harzburgites with $< \sim 2$ vol. % cpx grains, these grains could be a granular exsolution product developed from opx. However, this is less likely in rocks with more abundant cpx, say, significantly >2 vol. %. Importantly, the complementarity between cpx vol. % in abyssal peridotites and Na_8 (Na_2O normalized to MgO = 8·0 wt %) of spatially associated MORB (Niu *et al.*, 1997) suggests that most cpx grains in abyssal peridotites are indeed a residual phase instead of an exsolution product. Therefore, the trace element compositions reported for cpx are probably a characteristic of the residual cpx grains (at least the cores). However, we do not know if subsolidus re-equilibration may have any effect on REE redistribution in cpx. For example, can we rule out the possibility that residual cpx may have lost progressively lighter (greater ionic size) REE during subsolidus re-equilibration? The solubility of progressively lighter REE in cpx may decrease with falling temperature. This can be tested by *in situ* LA-ICP-MS profile analyses of REE (and other incompatible elements) in the cpx of unserpentinized mantle melting residues to see if there is any spatial compositional gradient. Such a test is needed to evaluate the validity of interpretations based on cpx trace REE data (Hellebrand & Snow, 2003).

The geochemical effects of serpentinization vs seafloor weathering

The literature on serpentinization of mantle peridotites is abundant (e.g. Coleman, 1977; Seyfried & Dibble, 1980; Janecky & Seyfried, 1986; O'Hanley, 1996), and various models of isochemical and iso-volume reactions have been proposed. It is likely in practice that volume expansion is inevitable during serpentinization because of the formation of low-density serpentines [$\sim 2{\cdot}3\ g/cm^3$ for Mg end-member $Mg_3Si_2O_5(OH)_4$ despite the production of dense magnetite trails or aggregates] from the dense peridotite minerals (all $> 3{\cdot}2\ g/cm^3$). Indeed, serpentinite diapirs (less dense and positively buoyant) have been observed to be tectonically important (e.g. Coleman, 1977; Nicolas, 1989; Cannat *et al.*, 1992; Cannat, 1993; Cannat & Casey, 1995). Serpentinization is certainly not isochemical at least in terms of water. As olivine is volumetrically far more abundant than opx and cpx in mantle peridotites, and because olivine is far more prone to serpentinization, we may infer from the Mg/Si = 2 ratio in forsterite olivine (Mg_2SiO_4) to Mg/Si = 1·5 in magnesian serpentine [$Mg_3Si_2O_5(OH)_4$] that Mg loss would be a natural consequence of serpentinization if no evidence exists for Si addition. The lost Mg could form brucite [$Mg(OH)_2$]; however, the latter is rarely observed in abyssal peridotites (Dick, 1989; Niu & Hékinian, 1997*b*). This reasoning supports the interpretation (see Fig. 2 and related discussion) that the analyzed bulk-rock abyssal peridotites reflect various extents of Mg loss with an average of ~10 wt % for the entire dataset. Although this interpretation is sensible, we cannot dismiss the obvious question of where on Earth the lost Mg may have gone to or been stored, and in what form. In fact, the 'Lost City' hydrothermal field on 1·5 Myr old ocean crust flanking the Mid-Atlantic Ridge at 30°N, which is the only hydrothermal field that is interpreted to be genetically associated with mantle peridotite serpentinization (Kelley *et al.*, 2001), has vent fluids with very low, not high, Mg (~3–6 times less than in seawater), consistent with peridotite-dominated fluid–rock interactions observed experimentally (Janecky & Seyfried, 1986; Wetzel & Shock, 2000). This suggests that near-ridge serpentinization is not associated with Mg loss. Perhaps,

the actual near-ridge serpentinization is buffered by the reaction: $2Mg_2SiO_4$ (Forsterite olivine) + $Mg_2Si_2O_6$ (Enstatite opx) + 4 H_2O = $2Mg_3Si_2O_5(OH)_4$ (Serpentine), which requires no Mg loss or Si gain (constant atomic ratio Mg/Si = 3/2), but addition of water. Therefore, it is possible that the apparent Mg loss in analyzed bulk-rock abyssal peridotites (Fig. 2), which are dredged from the seafloor, probably results from the seafloor weathering of serpentine (vs primary olivine and other peridotite minerals) (Snow & Dick, 1995).

If Mg is not as mobile as widely perceived during the serpentinization process, and because the bulk-rock MgO maintains melting systematics in terms of melting stoichiometry (Fig. 4) as well as correlated variations with moderately incompatible elements (Figs 5 and 11), it seems likely that serpentinization processes are close to isochemical for most elements considered (see Electronic Appendix 1) except for H_2O addition. Ca could be mobile, but there is no strong evidence (Fig. 3e). No rodingite mineral assemblage has been recognized in any of the studied samples. The significant correlations of LREE with HFSE (Fig. 8) and of Ti, Zr, Nb and Th with many other incompatible elements (Fig. 15) suggest that these elements are largely unaffected by serpentinization because their behaviors are like those predicted for magmatic systems (see above). These observations are important because they require a serious revision of our ideas about the geochemical consequences of serpentinization, particularly in terms of which elements may be mobile. We suspect that the alkali elements (Li, Na, K, Rb, Cs) and U and Sr, which show rather poor correlations with all other incompatible elements (Fig. 15), may be mobile during serpentinization. This suspicion, however, may not be correct. For example, U becomes water-soluble or mobile only when it occurs as U^{6+} under oxidizing conditions (vs U^{4+}, which is water-insoluble and immobile), yet serpentinization occurs under reduced conditions as evidenced by the formation of FeS, native Fe, FeNi and CoNi alloys (e.g. Frost, 1985; O'Hanley, 1996) as well as abundant H_2, H_2S and CH_4 (Kelley & Früh-Green, 1999; Kelley *et al.*, 2002). Under such highly reduced conditions, U should occur as U^{4+}, which cannot be water-soluble and mobile. Therefore, the variable and highly elevated abundances of U in bulk-rock abyssal peridotites cannot be gained during serpentinization, but must be added under more oxidizing conditions, which are most likely during seafloor weathering. As serpentinization fluids have about twice as much Ca as seawater (Kelley *et al.*, 2002), we can infer that Sr (which behaves like Ca geochemically) could be mobile during serpentinization and may have been leached out of the serpentinizing peridotites. Serpentinization is obviously open to seawater Na and Cl even though serpentines are neither a source nor a sink for these two elements because serpentinization fluids have essentially the same Na and Cl abundances as seawater (Kelley *et al.*, 2002).

Existing Sr and Nd isotopic data on abyssal peridotites are consistent with the interpretations presented here (Snow *et al.*, 1993, 1994; Wendt *et al.*, 1999; Salters & Dick, 2002). Sr is mobile during serpentinization and/or seafloor weathering, and $^{87}Sr/^{86}Sr$ values approach seawater values. On the other hand, Nd behaves as an immobile element, and $^{143}Nd/^{144}Nd$ values reflect MORB-source mantle values and sub-ridge magmatic processes.

More on melt–residue complementarity

The statistically significant correlation of residual cpx (vol. %) in abyssal peridotites with Na_8 of spatially associated MORB (Dick *et al.*, 1984; Niu *et al.*, 1997) provides the most convincing evidence that abyssal peridotites are MORB melting residues. With increasing extent of melting, Na, as a moderately incompatible element, decreases in the melt while cpx becomes progressively consumed or depleted in the residues. This interpretation is sensible. However, such complementarity could very well be inherited from fertile MORB-source compositional variation. For example, partial melting of a previously depleted source with low cpx abundances, thus low bulk-rock Na, should yield melts with less Na and even more cpx-depleted residues. Therefore, using Na_8 in MORB melts to infer the extent of mantle melting for MORB genesis and mantle potential temperature is at best an interesting exercise with little practical significance unless there exists independent evidence. The same is true in using spinel compositions and cpx REE to calculate the extent of melting (Hellebrand *et al.*, 2001).

Interpretations of cpx trace element data (Johnson *et al.*, 1990) in terms of extent of melting for MORB genesis also require an understanding of the fertile source compositional control. For example, Johnson *et al.* (1990) noted that residual cpx in abyssal peridotite samples dredged from near hotspots (e.g. Bouvet and Marion at the Southwest Indian Ridge) are more depleted in incompatible trace elements than samples dredged away from hotspots, which is interpreted to be consistent with higher extents of melting in hotspot-influenced mantle. However, we should also note that MORB samples from ridges near those same hotspots are more enriched in incompatible elements (e.g. LREE) than MORB samples away from the hotspots (Le Roex *et al.*, 1983, 1985). How could it be possible that incompatible elements are more enriched in MORB produced by greater extents of melting of a uniform mantle source? The answer is straightforward. The fertile MORB source materials near the hotspots are more enriched in incompatible elements than MORB source materials away from the hotspots. This suggests that the greater extent of melting or melt depletion near hotspots inferred from residual cpx

incompatible elements may not be due to a hot mantle, but because of a compositionally more fertile, and thus, more fusible mantle. Enriched mantle with elevated abundances of incompatible elements, and in particular alkalis and volatiles, will lead to greater extents of melting because of its lowered solidus (Niu *et al.*, 2001), producing incompatible element-enriched MORB but more depleted residues. Whether these hotspots (i.e. Bouvet and Marion) are hot or not is unknown, but we do know that the fertile mantle source near the hotspots is more enriched in incompatible elements and volatiles (Le Roex *et al.*, 1983, 1985).

The above suggests that incompatible elements (e.g. LREE) in MORB at these near-hotspot ridges are decoupled from major elements such as Na_2O. This has been observed in many ridges, in particular the Mid-Atlantic Ridge at ~14°N, where Na_2O is depleted yet other alkalis, volatiles (popping rocks) and incompatible elements are highly enriched (Bougault *et al.*, 1988). This is consistent with the source mantle being metasomatized with enriched dikes or veins dispersed in a more depleted harzburgitic matrix (Niu *et al.*, 1999, 2002*a*; Niu & O'Hara, 2003). The message is that we should note the importance of fertile mantle compositional (vs temperature) control on MORB petrological and geochemical characteristics.

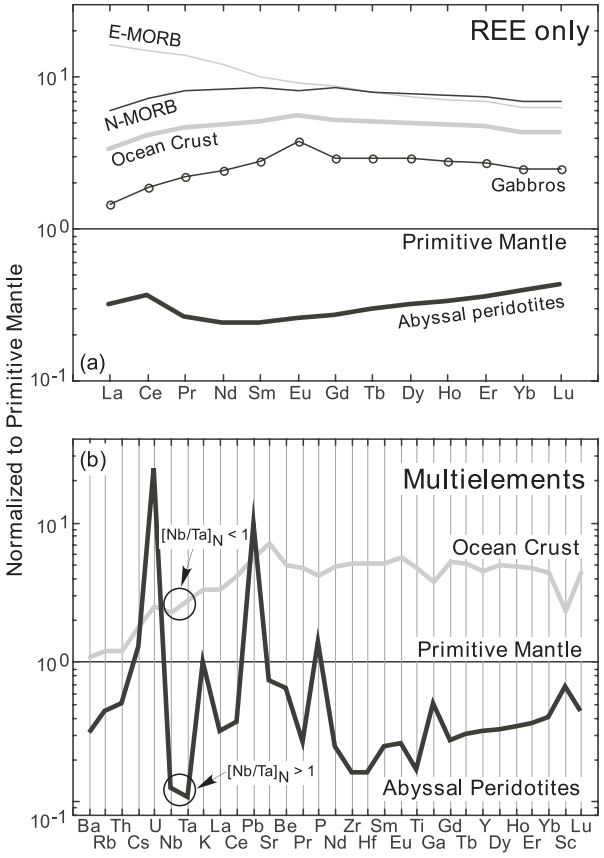

Fig. 19. Comparison of global average of abyssal peridotites with average depleted normal MORB (N-MORB), enriched MORB (E-MORB), oceanic gabbros and model ocean crust (Niu & O'Hara, 2003) in terms of REE (a) and other incompatible elements (b) on primitive mantle (Sun & McDonough, 1989; McDonough & Sun, 1995) normalized plots. The higher than expected abundances of more incompatible elements to the left should be noted; these support the suggestion that abyssal peridotites are not simple melting residues. Mobile elements such as Rb, Cs, U, K and Sr (see Fig. 15) may be added during serpentinization or seafloor weathering, but Ba, Th, Nb, Ta, Pb and LREE are enriched by post-melting magmatic processes. The subchondritic Nb/Ta ratio of model ocean crust and super-chondritic Nb/Ta ratio in average abyssal peridotites should also be noted.

Some implications for chemical geodynamics

The geochemical characteristics of individual peridotite samples or sample suites may be caused by many factors such as fertile source heterogeneity, alteration and seafloor weathering, as well as more recent melting and melt extraction events involved in ocean crust genesis. However, the 'global' averages should tell us the first-order systematics of the most important processes for a particular element or elements. That is, the less significant effects on those elements should be averaged out. With this in mind, we can discuss some possible implications of the data in the context of chemical geodynamics.

Eu anomalies

Figure 19a compares average bulk-rock compositions of abyssal peridotites with average normal and enriched MORB (N-MORB and E-MORB), oceanic lower-crustal gabbros, and model ocean crust (Niu *et al.*, 2002*a*, 2002*b*; Niu & O'Hara, 2003) on a primitive mantle normalized REE diagram. The overall lower REE abundances of abyssal peridotites than the primitive mantle values are consistent with these peridotites being melting residues. The LREE depletion of model ocean crust is consistent with the depleted fertile MORB source resulting from continental crust extraction in the Earth's early history (e.g. Armstrong, 1968; Gast, 1968; Jacobsen & Wasserburg, 1979; O'Nions *et al.*, 1979; DePaolo, 1980; Allègre *et al.*, 1983; Hofmann *et al.*, 1986). The weak positive Eu anomaly (~8%) of the model ocean crust may be real (not necessarily due to the gabbroic effect) because a positive Eu anomaly is common in most depleted and primitive MORB melts erupted or quenched at temperatures above the plagioclase liquidus (Niu & Batiza, 1997). The weak positive Eu anomaly may be inherited from the depleted fertile MORB mantle; Eu may have been preferentially left behind during previous melt extraction events because Eu^{2+} is probably not as incompatible as Sm^{3+} and Gd^{3+} during previous mantle

melting. The average ~4% negative Eu anomaly of average continental crust (Rudnick & Fountain, 1995) may very well complement the small positive Eu anomalies in the depleted fertile MORB-source mantle.

Some positive and negative Eu anomalies in bulk-rock abyssal peridotites (Fig. 6) are probably due to serpentinization or seafloor weathering as is the case for Sr. This interpretation is consistent with the poor Eu–Mg correlation (vs better Sm–Mg and Gd–Mg correlations) in Fig. 11. These 'individual' anomalies are averaged out (Fig. 19a).

Straightforward melting signals and signals of melt–residue interactions

Figure 19b compares average geochemical characteristics of model ocean crust and abyssal peridotites in a primitive mantle normalized multi-element diagram. The complementary relationships between the two for HREE (see Fig. 19a), Ga and Sc are expected as a result of mantle melting. Whereas the bulk of sub-ridge melting for ocean crust formation takes place in the spinel peridotite stability field, the HREE–Ga–Sc complementarity suggests the preservation or inheritance of some garnet signatures in abyssal peridotites; progressively heavier REE elements, and in particular Sc (perhaps also Ga?), are more compatible in garnet. A small positive Sr anomaly in the model ocean crust may be inherited from the fertile MORB source as may be the case for Eu, if the primitive mantle value for Sr (Sun & McDonough, 1989) is not too low. The number of significant anomalies in the trace element patterns of average abyssal peridotites is remarkable. If we accept the interpretation (see Fig. 15) that U, Sr, Rb, Cs and K are due mostly to seafloor weathering, then the elevated abundances of Ba, Th, Nb, Ta, LREE, Be, P, Zr and Hf with respect to the expected melting residues must be due to magmatic refertilization (see Figs 8–10 and 16). As the magmatic enrichments of these elements do not provide a 'smooth' pattern as predicted from MORB melts or model ocean crust, we can infer that the refertilization is a rather complex process. If the refertilization takes place in the TBL as ascending melts migrate through the advanced residues (Fig. 1), and if the melt–residue interaction is a chromatographic process (see Fig. 18), then the bulk distribution coefficients (bulk D values) of all these elements during the 'chromatographic' process must differ from their respective bulk D values during mantle partial melting. As the between-element fractionation is significant (e.g. Nb–Ta, Zr–Hf, Nb–Th, etc.), it is expected that such 'chromatographic' processes must be characteristic of very low melt/rock ratios. Under such conditions, mass-dependent fractionation (such as Nb–Ta and Zr–Hf; see above) as a result of different diffusion or transport rates or other factors needs to be further investigated (see Fig. 18). For example, why are Ba and Th much more enriched than Nb and Ta? Why is Pb much more enriched, at levels higher than in the oceanic crust? If Pb is stored in sulfides, why does Pb correlate so well with the LREE and other highly incompatible elements such as Ba, Th and Nb (Fig. 16)? Answers to these questions require melt–solid interaction experiments at low melt/solid ratios.

Missing-Nb reservoir?

It should be noted that $[Nb/Ta]_N$ is <1 in the model ocean crust (Fig. 19b) (Niu & Batiza, 1997; Rudnick *et al.*, 2000), which is less than the chondritic Nb/Ta ratio of ~17·6. The subchondritic Nb/Ta ratio of both average continental crust (~12, Taylor & McLennan, 1985; Rudnick & Fountain, 1995) and average MORB melts (Niu & Batiza, 1997) has led to speculation about the existence of a missing Nb reservoir (see above). Of course, there would indeed be missing Nb if, and only if, the bulk Earth has a chondritic Nb/Ta ratio in the first place. If we assume a chondritic Earth composition, then the missing Nb must reside somewhere in the Earth. There may indeed be a hidden Nb-rich reservoir deep in the mantle (e.g. McDonough, 1991; Blichert-Toft & Albarède, 1997; Rudnick *et al.*, 2000; Albarède & van der Hilst, 2002; Niu & O'Hara, 2003) or perhaps in the Earth's core (Wade & Wood, 2001). The surprisingly large Nb–Ta (also Zr–Hf) fractionations in abyssal peridotites (Fig. 12) may be revealing. Perhaps such huge Nb–Ta and Zr–Hf fractionations are unique to abyssal peridotites. We cannot, however, rule out the possibility that such large fractionations may be widespread, at least atop the oceanic lithosphere as reflected by these peridotites. Although the overall Nb and Ta abundances are low in abyssal peridotites, the mean $[Nb/Ta]_N > 1$ (Fig. 19b) is intriguing. Given the mean Nb/Ta ~ 26 much greater than the chondritic value of ~17·6 (mean Zr/Hf ~ 45 greater than the chondritic value of ~36·3), and if the volume of the mantle with such degrees of fractionations is significant, then the 'missing Nb' must still be in the mantle. If Nb–Ta (also Zr–Hf) fractionation largely happens in the TBL beneath mid-ocean ridges and if the same process has been taking place since the operation of plate tectonics with Nb–Ta (also Zr–Hf) fractionated materials (topmost oceanic lithospheric mantle) returning to the deep mantle through subduction zones, we may predict more subchondritic materials to surface in the crust with time if crust–mantle recycling is not perfectly reversible. This hypothetical interpretation requires further testing, but the observations (Fig. 19b) need to be considered in terms of models of Nb–Ta fractionation in the context of chemical geodynamics.

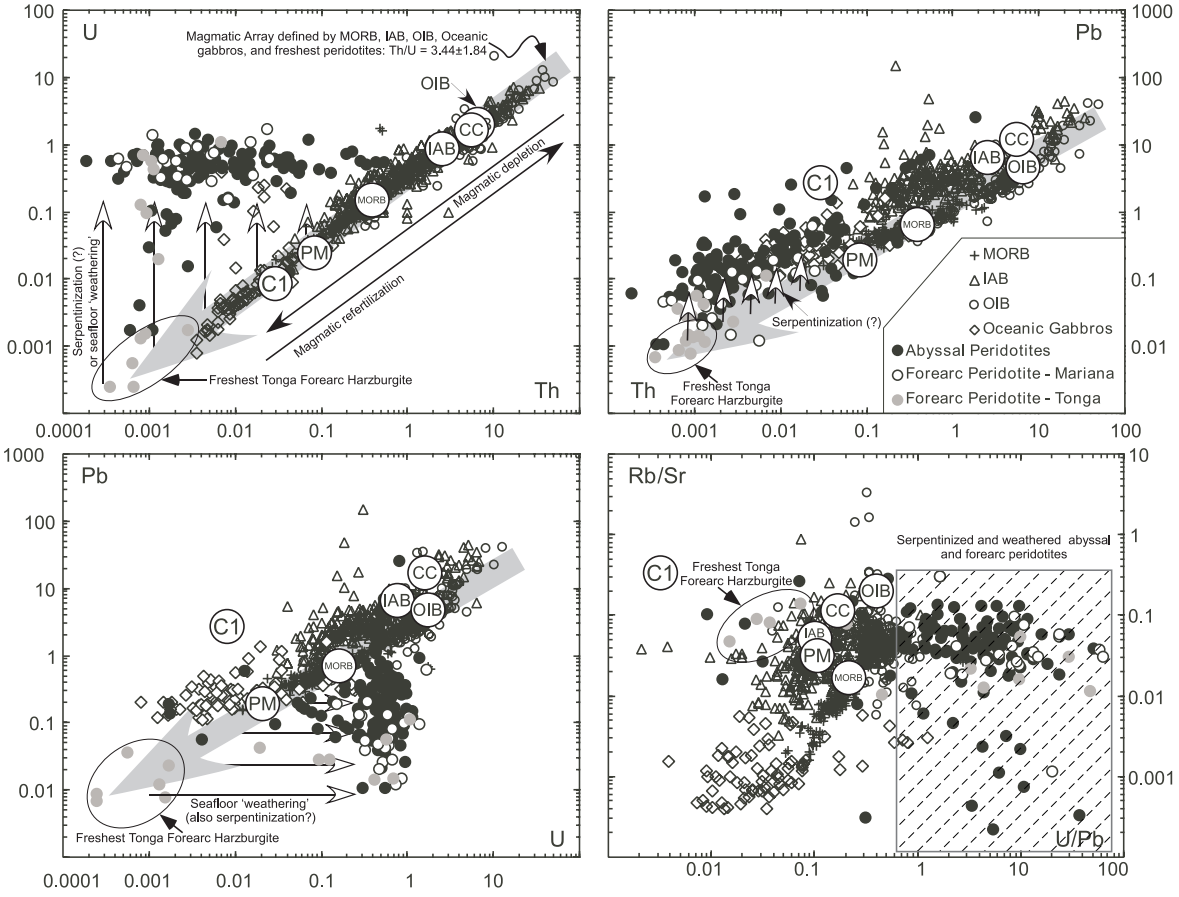

Fig. 20. Comparisons of abyssal peridotites with MORB, IAB (island arc basalts), OIB (ocean island basalts), oceanic gabbros, serpentinized Mariana forearc peridotites and both extremely fresh and serpentinized Tonga forearc peridotites in U–Th, Pb–Th, Pb–U and Rb/Sr–U/Pb spaces. Data sources: MORB, Niu *et al.* (1999, 2001, 2002*a*) and Regelous *et al.* (1999); IAB, Ewart *et al.* (1998) and Y. Niu (unpublished data, 2004) from Mariana and Tonga; OIB, M. Regelous (compiled data, 2002); oceanic gabbros, Bach *et al.* (2001), Niu *et al.* (2002*b*), Niu & O'Hara (2003) and Y. Niu (unpublished data, 2004); Mariana and Tonga forearc peridotites, Y. Niu (unpublished data, 2004). Open circles with letters are respective averages. Average OIB, PM and C1 values are from Sun & McDonough (1989), and CC (bulk continental crust) from Rudnick & Fountain (1995). Among all these elements, U, Rb and Sr are shown to be mobile (Fig. 15), and all have been added to the expected melting residues. In particular, the fresh unserpentinized Tonga forearc peridotites plot at the most depleted end of the magmatic U–Th array, yet serpentinized and weathered abyssal and forearc peridotites are highly enriched in U, leading to elevated U/Pb ratios. Of all the lithologies considered, serpentinized and weathered abyssal peridotites (also forearc peridotites) have the highest U/Pb.

Possible consequences of serpentinized-seafloor subduction

This is a rather complex topic that involves poorly understood details of the geochemical consequences of subduction-zone metamorphism. A detailed account is beyond the scope of this contribution. However, a comparison of serpentinized or weathered abyssal peridotites with other major oceanic lithologies (except for sediments) that have subduction potential may provide some insights into the origin and diversity of mantle compositional and isotopic heterogeneities (Fig. 20). The following discussion assumes that subduction zone dehydration is incomplete. This assumption is reasonable because serpentines (containing up to 13 wt % water) can be stable up to 7 GPa (at $T < 700$°C; Ulmer & Trommsdorff, 1995) before being transformed to dense hydrous magnesium silicate phases (DHMS: A, B, D–F–G and G) at greater pressures (~5–50 GPa) (e.g. Frost, 1999; Williams & Hemley, 2001). These phases would carry not only a large quantity of water (~3–20 wt %) but probably also chemical elements characteristic of the serpentines (e.g. Figs 19 and 20) into the deep mantle (Kuroda & Irifune, 1998).

Figure 20 compares serpentinized and weathered abyssal peridotites with MORB, island arc basalts (IAB), ocean island basalts (OIB), oceanic gabbros, serpentinized Mariana forearc peridotites, and both fresh and serpentinized Tonga forearc peridotites in U–Th, Pb–Th, Pb–U and Rb/Sr–U/Pb spaces. The fresh Tonga forearc peridotites plot at the most depleted end of the magmatic trends defined by basaltic rocks in U–Th, Pb–Th and Pb–U spaces, but abyssal peridotites and serpentinized

and weathered forearc peridotites have elevated abundances of U (to a lesser extent Pb). In Rb/Sr vs U/Pb space, abyssal peridotites and serpentinized and weathered forearc peridotites have variably higher U/Pb ratios (1–70) than any other oceanic rocks and fresh forearc peridotites yet have relatively low Rb/Sr ratios (0·0003–0·15). If such geochemical signatures in serpentinized peridotites are preserved along with H_2O in these rocks transported deep into the mantle (see above), serpentinized and weathered seafloor peridotites may be the most promising sources that contribute to the HIMU isotopic signatures of some OIB. Subduction of oceanic lithosphere with a subduction-zone processed crust on the top, with serpentinized seafloor peridotites (including possible deep serpentinization at the trench–outer-rise) in the middle and with a low-velocity-zone metasomatized peridotite section at the base (Niu & O'Hara, 2003) will undoubtedly contribute to small-scale and large-amplitude compositional heterogeneities in the Earth's mantle (Niu *et al.*, 1999, 2002*a*).

SUMMARY

(1) This paper presents the very first bulk-rock major and trace element data on ~130 abyssal peridotite samples from the Pacific and Indian ocean ridge–transform systems. The data reveal a number of surprises about the petrogenesis of these rocks, mantle melting and melt extraction processes beneath mid-ocean ridges, and elemental behaviors yet to be understood. The data, when considered in a global context, have far-reaching implications.

(2) Although abyssal peridotites are variably serpentinized, and may have also experienced seafloor weathering, magmatic signatures remain well preserved in bulk-rock compositions in terms of most major and trace elements, even though there is some obvious MgO loss, probably because of seafloor weathering.

(3) Despite some obvious MgO loss, the better inverse correlation of MgO with progressively heavier REE is consistent with bulk-rock cpx control, and thus, in general, with the extent of melt depletion. The latter, particularly as reflected in HREE, may either result from recent sub-ridge mantle melting or be inherited from MORB-source variations as a result of previous melt extraction events.

(4) LREE in bulk-rock samples are significantly more enriched, not more depleted, than in the constituent residual cpx of the same sample suites previously studied. If the residual cpx records recent sub-ridge mantle melting, then the bulk-rock LREE reflect post-melting refertilization. The significant correlations of LREE (i.e. La, Ce, Pr, Nd) with HFSE (e.g. Nb and Zr) indicate that the enrichments of both LREE and HFSE resulted from a common magmatic process, not serpentinization or seafloor weathering. The refertilization takes place in the 'cold' TBL beneath mid-ocean ridges, where the ascending melts migrate through and interact with the advanced residues. The magmatic refertilization did not affect the cpx relics that were analyzed for trace elements. It is possible that the ascending melts that percolate along grain boundaries in the TBL might affect only the cpx rims, which were subsequently serpentinized, and thus not analyzed for trace elements.

(5) The over two orders of magnitude variations in Zr/Hf and Nb/Ta ratios are unexpected. The statistically significant correlation between the two ratios ($R_{Nb/Ta–Zr/Hf} = 0{\cdot}698$ with $N > 130$) is consistent with the observations in basalts and experimental data that $D_{Zr} < D_{Hf}$ and $D_{Nb} < D_{Ta}$. However, we do not really understand yet in theory why $D_{Zr}/D_{Hf} < 1$ and $D_{Nb}/D_{Ta} < 1$ should be the case because of (a) the identical charges (5^+ for Nb and Ta and 4^+ for Zr and Hf) and (b) essentially the same ionic radii ($R_{Nb}/R_{Ta} = 1{\cdot}000$ and $R_{Zr}/R_{Hf} = 1{\cdot}006–1{\cdot}026$ for coordination numbers of 6, 7, 8 and 12) of the two elemental pairs. Considering the observation that for two elements of 'identical' chemical properties, the lighter one is more incompatible than the heavier one (mass ratios: $M_{Zr}/M_{Hf} = 0{\cdot}511$ and $M_{Nb}/M_{Ta} = 0{\cdot}513$) allows the hypothesis that mass-dependent diffusion or mass-transfer rates may play an important role in causing Nb–Ta and Zr–Hf fractionations. This hypothesis needs testing.

(6) Whereas the correlated Nb/Ta–Zr/Hf variation in seafloor basalts is mostly inherited from fractionated ratios in their mantle sources related to previous melting and enrichment events, it is hypothesized that the large Nb/Ta and Zr/Hf fractionations in abyssal peridotites result from a chromatographic process during melt ascent through advanced residues in the TBL under conditions of very low melt/rock ratios. There is the possibility that some 'exotic' phases with fractionated Nb/Ta and Zr/Ha ratios may preexist in the MORB mantle sources that survived from recent melting events. All these hypotheses need testing.

(7) The observations that the post-melting magmatic refertilization of the advanced residues in the TBL did not affect the relics of cpx previously studied, and that excess olivine (observed on thin-section scales) crystallized from the ascending cooling melts suggest that abyssal peridotites record snapshots of porous melt flow (along grain boundaries) in the TBL beneath mid-ocean ridges. Channeled flows inferred from dunite dikes or veins in ophiolites may be important, but abyssal peridotites are arguably materials sampled away from those probable dunite dikes or veins.

(8) Although the complementarity between modes (cpx vol. %) and mineral compositions (Mg-number of olivine, opx and cpx, and Cr-number of spinel) of abyssal peridotites and compositions (e.g. Na_8) of spatially

associated MORB suggest that abyssal peridotites are melting residues of MORB (not simple residues though), there is no clear justification that Na_8 in MORB or cpx mode in abyssal peridotites genuinely reflects the extent of mantle melting beneath mid-ocean ridges, nor that such inferred extent of melting reflects sub-ridge mantle potential temperature variations. The complementarity could very well be inherited from the fertile mantle sources. Caution is thus necessary when using MORB compositions to interpret the extent of sub-ridge mantle melting and mantle potential temperature.

(9) Serpentinization and seafloor weathering have not obliterated the magmatic signatures in the bulk-rock compositions of abyssal peridotites. This by no means suggests that no elements have been mobilized, but does suggest that the spatial scale of the mobility is not significantly greater than the size of samples studied. It is possible that the observed geochemical scattering may be significantly reduced if the size of the samples available for study is larger. Rb, Cs, K, Sr and U are obviously mobile, probably as a result of seafloor weathering.

(10) Abyssal peridotites have very high U abundances and the highest U/Pb ratios (~1–70) among oceanic rocks. If subduction zone dehydration is incomplete, then subduction of these rocks into deep mantle may contribute to the HIMU signatures in some OIB sources.

ACKNOWLEDGEMENTS

I am honored to contribute to the special volume in honor of Michael J. O'Hara for his tremendous scientific contributions to our field in understanding the petrogenesis of mafic and ultramafic rocks on the Earth and its Moon. Numerous stimulating discussions Mike and I have had during my Cardiff years (2001–2003) and ever since are always valuable and remembered. I sincerely thank Roger Hékinian, Bob Fisher, Henry Dick and Pat Castillo for their generosity in providing samples for this study. I thank the Australian Research Council for support for the analytical work done during my tenure at The University of Queensland. Kathleen Mahoney and Peter Colls are thanked for helping with sample preparation and making thin sections. Robert Cirocco and Alan Greig are thanked for analytical assistance. I also thank the University of Houstan, Beijing University and the National Science Foundation of China for support during the preparation and finalization of the paper. Discussion with Wolfgang Bach, Henry Dick, Fred Frey, Dave Green, Roger Hékinian, Claude Herzberg, Bill McDonough and Mike O'Hara has been helpful. Journal reviewers Wolfgang Bach, Jim Natland and an anonymous one are thanked for their constructive comments on an early version of the manuscript. Constructive comments and great editorial effort by Marjorie Wilson and Alastair Lumsden have improved the paper significantly, for which, and for their exceptional patience, I am grateful.

SUPPLEMENTARY DATA

Supplementary data for this paper are available at *Journal of Petrology* online.

REFERENCES

Aharonov, E., Spiegelman, M. & Kelemen, P. (1997) Three-dimensional flow and reaction in porous media: implications for the Earth's mantle and sedimentary basins. *Journal of Geophysical Research* **101**, 14821–14831.

Albarède, F. (1992). How deep do common basaltic magmas form and differentiate? *Journal of Geophysical Research* **97**, 10997–11009.

Albarède, F. & van der Hilst, R. D. (2002). Zoned mantle convection. *Philosophical Transactions of the Royal Society of London* **360**, 2569–2592.

Allègre, C. J., Hart, S. R. & Minster, J.-F. (1983). Chemical structure and evolution of the mantle and continents determined by inversion of Nd and Sr isotopic data, I. Theoretical methods. *Earth and Planetary Science Letters* **66**, 177–190.

Armstrong, R. L. (1968). A model for the evolution of strontium and lead isotopes in a dynamic earth. *Review of Geophysics and Space Physics* **6**, 175–200.

Asimow, P. D. (1999). A model that reconciles major- and trace-element data from abyssal peridotites. *Earth and Planetary Science Letters* **169**, 303–319.

Asimow, P. D., Hirschmann, M. M., Ghiorso, M. S., O'Hara, M. J. & Stolper, E. (1995). The effect of pressure-induced solid–solid phase transitions on decompression melting of the mantle. *Geochimica et Cosmochimica Acta* **59**, 4489–4506.

Asimow, P. D., Hirschmann, M. M. & Stolper, E. M. (2001). Calculation of peridotite partial melting from thermodynamic models of minerals and melts, IV. Adiabatic decompression and the composition and mean properties of mid-ocean ridge basalts. *Journal of Petrology* **42**, 963–998.

Bach, W., Alt, J. C., Niu, Y., Humphris, S. E., Erzinger, J. & Dick, H. J. B. (2001). The chemical consequences of late-stage hydrothermal circulation in an uplifted block of lower ocean crust at the Southwest Indian Ridge: results from ODP Hole 735B (Leg 176). *Geochimica et Cosmochimica Acta* **65**, 3267–3287.

Baker, M. B. & Beckett, J. R. (1999). The origin of abyssal peridotites: a reinterpretation of constraints based on primary bulk compositions. *Earth and Planetary Science Letters* **171**, 49–61.

Baker, M. B. & Stolper, E. M. (1994). Determining the composition of high-pressure mantle melts using diamond aggregates. *Geochimica et Cosmochimica Acta* **58**, 2811–2827.

Batiza, R. & Niu, Y. (1992). Petrology and magma chamber processes at the East Pacific Rise ~9°30′N. *Journal of Geophysical Research* **97**, 6779–6797.

Blichert-Toft, J. & Albarède, F. (1997). The Lu–Hf isotope geochemistry of chondrites and evolution of the mantle–crust system. *Earth and Planetary Science Letters* **148**, 243–258.

Blundy, J. & Wood, B. (1994). Prediction of crystal–melt partition coefficients from elastic moduli. *Nature* **372**, 452–454.

Bodinier, J.-L., Merlet, C., Bendini, R. M., Siemen, F., Ramaidi, M. & Garrido, C. J. (1996). Distribution of niobium and tantalum and

other highly incompatible trace elements in the lithospheric mantle: the spinel paradox. *Geochimica et Cosmochimica Acta* **60**, 545–550.

Bougault, H., Joron, J. L. & Treuil, M. (1979). Alteration, fractional crystallization, partial melting, mantle properties from trace elements in basalts recovered in the North Atlantic. In: Talwani, M., Harrison, C. G. & Hayes, D. E. (eds) *Deep Drilling Results in the North Atlantic: Ocean Crust. American Geophysical Union Maurice Ewing* **2**, 352–368.

Bougault, H., Dmitriev, L., Schilling, J.-G., Sobolev, A., Jordan, J. L. & Needham, H. D. (1988). Mantle heterogeneity from trace elements: MAR triple junction near 14°N. *Earth and Planetary Science Letters* **88**, 27–36.

Brandon, A. D, Snow, J. E., Walker, R. J., Morgan, J. W. & Mock, T. D. (2000). ^{190}Pt–^{186}Os and ^{187}Re–^{187}Os systematics of abyssal peridotites. *Earth and Planetary Science Letters* **177**, 319–335.

Braun, M. G. & Kelemen, P. B. (2002). Dunite distribution in the Oman Ophiolite: implications for melt flux through porous dunite conduits. *Geochemistry, Geophysics, Geosystems* **11**, 8603, doi:10.1029/2001GC000289.

Cannat, M. (1993). Emplacement of mantle rocks in the seafloor at mid-ocean ridges. *Journal of Geophysical Research* **98**, 4163–4172.

Cannat, M. & Casey, J. F. (1995). An ultramafic lift at the Mid-Atlantic Ridge: successive stages of magmatism in serpentinized peridotites from the 15°N region. In: Vissers, R. L. M. & Nicolas, A. (eds) *Mantle and Lower Crust Exposed in Oceanic Ridges and Ophiolites*. Dordrecht: Kluwer Academic, pp. 5–34.

Cannat, M., Bideau, D. & Bougault, H. (1992). Serpentinized peridotites and gabbros in the Mid-Atlantic Ridge axial valley at 15°37′N and 16°52′N. *Earth and Planetary Science Letters* **109**, 87–106.

Castillo, P. R., Natland, J. H., Niu, Y. & Lonsdale, P. (1998). Sr, Nd, and Pb isotopic variation along the Pacific ridges from 53 to 56°S: implications for mantle and crustal dynamic processes. *Earth and Planetary Science Letters* **154**, 109–125.

Coleman, R. G. (1977). *Ophiolites*. New York: Springer, 230 pp.

DePaolo, D. J. (1980). Crustal growth and mantle evolution: inferences from models of element transport and Nd and Sr isotopes. *Geochimica et Cosmochimica Acta* **44**, 1185–1196.

Dick, H. J. B. (1989). Abyssal peridotites, very slow spreading ridges and ocean ridge magmatism. In: Saunders, A. D. & Norry, M. J. (eds) *Magmatism in the Ocean Basins. Geological Society, London, Special Publications* **42**, 71–105.

Dick, H. J. B. & Fisher, R. L. (1984). Mineralogic studies of the residues of mantle melting: abyssal and alpine-type peridotites. In: Kornprobst, J. (ed.) *The Mantle and Crustal–Mantle Relationships—Mineralogical, Petrological, and Geodynamic Processes of the Third International Kimberlite Conference, Vol. II*. New York: Elsevier, pp. 295–308.

Dick, H. J. B. & Natland, J. H. (1996). Late-stage melt evolution and transport in the shallow mantle beneath the East Pacific Rise. In: Mével, C., Gills, K. M. & Allan, J. F. (eds) *Proceedings of the Ocean Drilling Program, Scientific Results, 147*. College Station, TX: Ocean Drilling Program, pp. 103–134.

Dick, H. J. B., Fisher, R. L. & Bryan, W. B. (1984). Mineralogical variability of the uppermost mantle along mid-ocean ridges. *Earth and Planetary Science Letters* **69**, 88–106.

Dick, H. J. B. & Shipboard Party of Leg 176 (2000). A long in situ section of the lower ocean crust: results of ODP Leg 176 drilling at the Southwest Indian Ridge. *Earth and Planetary Science Letters* **179**, 31–51.

Dick, H. J. B., Ozawa, K., Meyer, P. S., Niu, Y., Robinson, P. T., Constantin, M., Herbert, R., Natland, J., Hirth, G. & Mackie, S. (2002). Primary silicate mineral chemistry of a 1·5-km section of very-slow spread lower ocean crust: ODP Hole 735B, Southwest Indian Ridge. In: Natland, J. H., Dick, H. J. B., Miller, D. J. & Von Herzen, R. P. (eds) *Proceedings of the Ocean Drilling Program, Scientific Results, 176*, 60 pp. [Online]. Available at http://www-odp.tamu.edu/publications/176_SR/chap_10/chap_10.htm. Accessed August 2004.

Eggins, S. M., Woodhead, J. D., Kinsley, L. P. J., Mortimer, G. E., Sylvester, P., McCulloch, M. T., Hergt, J. M. & Handler, M. R. (1997). A simple method for the precise determination of >40 trace elements in geological samples by ICPMS using enriched isotope internal standardization. *Chemical Geology* **134**, 311–326.

Eggins, S. M., Rudnick, R. L. & McDonough, W. F. (1998). The composition of peridotites and their minerals: a laser-ablation ICP-MS study. *Earth and Planetary Science Letters* **154**, 53–71.

Elderfield, H. & Greaves, M. J. (1982). The rare earth elements in seawater. *Nature* **296**, 214–219.

Elliott, T., Plank, T., Zindler, A., White, W. & Bourdon, B. (1997). Element transport from slab to volcanic front at the Mariana Arc. *Journal of Geophysical Research* **102**, 14991–15019.

Elthon, D. (1992). Chemical trends in abyssal peridotites: refertilization of depleted oceanic mantle. *Journal of Geophysical Research* **97**, 9015–9025.

Engel, C. G. & Fisher, R. L. (1969). Lherzolite, anorthosite, gabbro, and basalt dredged from the mid-Indian Ocean ridge. *Science* **166**, 1136–1141.

Engel, C. G. & Fisher, R. L. (1975). Granitic to ultramafic rock complexes of the Indian Ocean ridge system, western Indian Ocean. *Geological Society of America Bulletin* **86**, 1553–1578.

Ewart, A., Collerson, K. D., Regelous, M., Wendt, J. I. & Niu, Y. (1998). Geochemical evolution within the Tonga–Kermadec–Lau arc–backarc system: the role of varying mantle wedge composition in space and time. *Journal of Petrology* **39**, 331–368.

Falloon, T. J. & Green, D. H. (1988). Anhydrous partial melting of peridotite from 8 to 35 kb and the petrogenesis of MORB. *Journal of Petrology, Special Lithosphere Issue*, 379–414.

Fang, N. & Niu, Y. (2003). Late Paleozoic ultramafic lavas in Yunnan, SW China, and their geodynamic significance. *Journal of Petrology* **44**, 141–158.

Fisher, R. L., Henry, H. J. B., Natland, J. H. & Meyer, P. S. (1987). Mafic/ultramafic suites of the slow spreading Southwest Indian Ridge: Protea exploration of the Antarctic plate boundary, 24°E–47°E. *Ofioliti* **11**, 147–178.

Foley, S. F., Matthias, G. B. & Jenner, G. A. (1999). Rutile/melt partition coefficients for trace elements and an assessment of the influence of rutile on the trace element characteristics of subduction zone magmas. *Geochimica et Cosmochimica Acta* **64**, 933–938.

Foley, S., Tiepolo, M. & Vannucci, R. (2002). Growth of early continental crust controlled by melting of amphibolite in subduction zones. *Nature* **417**, 837–840.

Forsyth, D. W. & The MELT Seismic Team (1998). Imaging the deep seismic structure beneath a mid-ocean ridge: the MELT experiment. *Science* **280**, 1215–1218.

Frey, F. A. (1969). Rare earth abundances in a high-temperature peridotite intrusion. *Geochimica et Cosmochimica Acta* **33**, 1429–1447.

Frey, F. A., Suen, C. J. & Stockman, H. (1985). The Ronda high temperature peridotite: geochemistry and petrogenesis. *Geochimica et Cosmochimica Acta* **49**, 2469–2491.

Frost, B. R. (1985). On the stability of sulfides, oxides, and native metals in serpentine. *Journal of Petrology* **26**, 31–63.

Frost, D. J. (1999). The stability of dense hydrous magnesium silicates in Earth's transition zone and lower mantle. In: Fei, Y., Bertka, C. M. & Mysen, B. O. (eds) *Mantle Petrology: Field Observations and High Pressure Experimentation—a Tribute to Francis R. (Joe) Boyd. Geochemical Society Special Publication* **6**, 241–258.

Gast, P. W. (1968). Trace element fractionation and the origin of tholeiitic and alkaline magma types. *Geochimica et Cosmochimica Acta* **32**, 1055–1086.

Godard, M., Jousselin, D. & Bodinier, J. L. (2000). Relationship between geochemistry and structure beneath a paleo-spreading centre: a study of the mantle section of the Oman ophiolite. *Earth and Planetary Science Letters* **180**, 133–148.

Green, T. H., Blundy, J. D., Adam, A. & Yaxley, G. M. (2000). SIMS determination of trace element partition coefficients between garnet, clinopyroxene and hydrous basaltic liquids at 2–7·5 GPa and 1080–1200°C. *Lithos* **53**, 165–187.

Griselin, M. & Davies, G. R. (2003). The major element composition of unaltered peridotites: implications for the nature of partial melting. *Geophysics Research Abstract* **5**, 02201.

Grove, T. L., Kinzler, R. J. & Bryan, W. B. (1992). Fractionation of mid-ocean ridge basalts (MORB). In: Phipps Morgan, J., Blackman, D. K. & Sinton, J. M. (eds) *Mantle Flow and Melt Generation at Mid-ocean Ridges. Geophysical Monograph, American Geophysical Union* **71**, 281–310.

Hart, S. R. & Zindler, A. (1986). In search of bulk Earth composition. *Chemical Geology* **57**, 247–267.

Hauri, E. H., Wagner, T. P. & Grove, T. L. (1994). Experimental and natural partitioning of Th, U, Pb and other trace elements between garnet, clinopyroxene and basaltic melts. *Chemical Geology* **117**, 149–166.

Hellebrand, E. & Snow, J. E. (2003). A correction for subsolidus exsolution effects on trace elements in clinopyroxenes of abyssal peridotites. *Geophysical Research Abstracts* **5**, 03177.

Hellebrand, E., Snow, J. E., Dick, H. J. B. & Hofmann, A. W. (2001). Coupled major and trace elements as indicators of the extent of melting in mid-ocean-ridge peridotites. *Nature* **410**, 677–681.

Hirschmann, M. M. & Stolper, E. M. (1996). A possible role for garnet pyroxenite in the origin of the 'garnet signature' in MORB. *Contributions to Mineralogy and Petrology* **124**, 185–208.

Hirschmann, M. M., Ghiorso, M. S. & Stolper, E. M. (1999). Calculation of peridotite partial melting from thermodynamic models of minerals and melts. II. Isobaric variations in melts near the solidus and owing to variable source composition. *Journal of Petrology* **40**, 297–313.

Hofmann, A. W. (1988). Chemical differentiation of the Earth: the relationship between mantle, continental crust, and oceanic crust. *Earth and Planetary Science Letters* **90**, 297–314.

Hofmann, A. W. (1997). Mantle geochemistry: the message from oceanic volcanism. *Nature* **385**, 219–229.

Hofmann, A. W., Jochum, K. P., Seufert, M. & White, W. M. (1986). Nb and Pb in oceanic basalts: new constraints on mantle evolution. *Earth and Planetary Science Letters* **79**, 33–45.

Jacobsen, S. B. & Wasserburg, G. J. (1979). The mean age of mantle and crustal reservoirs. *Journal of Geophysical Research* **84**, 7411–7427.

Jagoutz, E., Palme, H., Blum, H., Cendales, M., Dreibus, G., Spettel, B., Lorenz, V. & Wänke, H. (1979). The abundances of major, minor and trace elements in the Earth's mantle as derived from primitive ultramafic nodules. *Proceeding of 10th Lunar Planetary Science Conference. Geochimica et Cosmochimica Acta Supplement 10*, 2031–2051.

Janecky, D. R. & Seyfried, W. E. (1986). Hydrothermal serpentinization of peridotite within the oceanic crust: experimental investigations of mineralogy and major element chemistry. *Geochimica et Cosmochimica Acta* **50**, 1357–1378.

Jaques, A. L. & Green, D. H. (1980). Anhydrous melting of peridotite at 0–15 kb pressure and the genesis of tholeiitic basalts. *Contributions to Mineralogy and Petrology* **73**, 287–310.

Jochum, K. P., Seufert, H. M., Spettel, B. & Palme, H. (1986). The solar-system abundances of Nb, Ta and Y and the relative abundances of refractory lithophile elements in differentiated planetary bodies. *Geochimica et Cosmochimica Acta* **50**, 1173–1183.

Jochum, K. P., Hofmann, A. W., Seufert, M., Stoll, B. & Polat, A. (2002). Niobium in planetary cores: consequences for the interpretation of terrestrial Nb systematics. *EOS Transactions, American Geophysical Union* **83**, F1446.

Johnson, K. T. M. & Dick, H. J. B. (1992). Open system melting and the temporal and spatial variation of peridotite and basalt compositions at the Atlantis II F. Z. *Journal of Geophysical Research* **97**, 9219–9241.

Johnson, K. T. M., Dick, H. J. B. & Shimizu, N. (1990). Melting in the oceanic upper mantle: an ion microprobe study of diopside in abyssal peridotites. *Journal of Geophysical Research* **95**, 2661–2678.

Kelemen, P. B., Shimizu, N. & Salters, V. J. (1995). Extraction of mid-ocean-ridge basalt from the upwelling mantle by focused flow of melt in dunite channels. *Nature* **375**, 747–753.

Kelemen, P. B., Hirth, G., Shimizu, N., Spiegelman, M. & Dick, H. J. B. (1997). A review of melt migration processes in the adiabatically upwelling mantle beneath oceanic ridges. *Philosophical Transactions of the Royal Society of London, Series A* **355**, 67–102.

Kelley, D. S. & Früh-Green, G. L. (1999). Abiogenic methane in deep-seated mid-ocean ridge environments: insights from stable isotope analyses. *Journal of Geophysical Research* **104**, 10439–10460.

Kelley, D. S., Karson, J. A., Blackman, D. K., Fruh-Green, G. L., Butterfield, D. A., Lilley, M. D., Olson, E. J., Schrenk, M. O., Roe, K. K., Lebon, G. T. & Rivizzigno, P. (2001). An off-axis hydrothermal vent field near the Mid-Atlantic Ridge at 30°N. *Nature* **412**, 145–149.

Kelley, D. S., Baross, J. A. & Delaney, J. R. (2002). Volcanoes, fluids, and life at mid-ocean ridge spreading centers. *Annual Review of Earth and Planetary Sciences* **30**, 385–491.

Kinzler, R. J. & Grove, T. L. (1992). Primary magmas of mid-ocean ridge basalts, 2, applications. *Journal of Geophysical Research* **97**, 6907–6926.

Klein, C. & Hurlbut, C. S., Jr (1999). *Manual of Mineralogy* (after J. D. Dana), revised 21st edn. New York: John Wiley, 681 pp.

Klein, E. M. & Langmuir, C. H. (1987). Global correlations of ocean ridge basalt chemistry with axial depth and crustal thickness. *Journal of Geophysical Research* **92**, 8089–8115.

Klemme, S., Blundy, J. D. & Wood, B. J. (2002). Experimental constraints on major and trace element partitioning during partial melting of eclogite. *Geochimica et Cosmochimica Acta* **66**, 3109–3123.

Kogiso, T., Tatsumi, Y. & Nakano, S. (1997). Trace element transport during dehydration processes in the subducted oceanic crust: 1. Experiments and implications for the origin of ocean island basalts. *Earth and Planetary Science Letters* **148**, 193–205.

Korenaga, J. & Kelemen, P. B. (1997). Melt migration through the oceanic lower crust: a constraint from melt percolation modeling with finite solid diffusion. *Earth and Planetary Science Letters* **156**, 1–11.

Kuroda, K. & Irifune, T. (1998). Observation of phase transformations in serpentine at high pressure and high temperature by in situ X-ray diffraction measurements. In: Manghnani, M. H. & Yagi, T. (eds) *Properties of Earth and Planetary Materials. American Geophysical Union Monograph* **101**, 545–554.

Kwiecien, W. (1990). *Silicate Rock Analysis by AAS.* Brisbane, QLD: School of Geology, Queensland University Technology.

Langmuir, C. H. (1989). Geochemical consequences of in situ crystallization. *Nature* **340**, 199–205.

Langmuir, C. H., Klein, E. M. & Plank, T. (1992). Petrological systematics of mid-ocean ridge basalts: constraints on melt generation beneath ocean ridges. In: Phipps Morgan, J., Blackman, D. K.

& Sinton, J. M. (eds) *Mantle Flow and Melt Generation at Mid-ocean Ridges. American Geophysical Union Monograph* **71**, 183–280.

Lasaga, A. C. (1998). *Kinetic Theory in the Earth Sciences*. Princeton, NJ: Princeton University Press, 811 pp.

Lee, C.-T. A., Brandon, A. D. & Norman, M. (2003). Vanadium in peridotites as a proxy for paleo-fO_2 during partial melting: prospects, limitations, and implications. *Geochimica et Cosmochimica Acta* **67**, 3045–3064.

Le Roex, A. P., Dick, H. J. B., Erlank, A. L., Reid, A. M., Frey, F. A. & Hart, S. R. (1983). Geochemistry, mineralogy and petrogenesis of lavas erupted along the Southwest Indian Ridge between the Bouvet Triple Junction and 11 degrees east. *Journal of Petrology* **24**, 267–318.

Le Roex, A. P., Dick, H. J. B., Erlank, A. L., Reid, A. M., Frey, F. A. & Hart, S. R. (1985). Petrology and geochemistry of basalts from the American–Antarctic Ridge, Southern Ocean: implications for the westward influence of the Bouvet mantle plume. *Contributions to Mineralogy and Petrology* **90**, 367–380.

Lindsley, D. H. & Anderson, D. J. (1983). A two-pyroxene thermometer. *Proceedings of the 13th Lunar and Planetary Science Conference, Part 2. Journal of Geophysical Research* **88**, Supplement, A887–A906.

Lundstrom, C. C. (2000). Rapid diffusive infiltration of sodium into partially molten peridotite. *Nature* **403**, 527–530.

Lundstrom, C. C., Gill, J., Williams, Q. & Perfit, M. R. (1995). Mantle melting and basalt extraction by equilibrium porous flow. *Science* **270**, 1958–1961.

McDonough, W. F. (1991). Partial melting of subducted oceanic crust and isolation of its residual eclogitic lithology. *Philosophical Transactions of the Royal Society of London, Series A* **335**, 407–418.

McDonough, W. F. & Sun, S.-s. (1995). The composition of the Earth. *Chemical Geology* **120**, 223–253.

McKenzie, D. & Bickle, M. J. (1988). The volume and composition of melt generated by extension of the lithosphere. *Journal of Petrology* **29**, 625–679.

Michael, P. J. & Bonatti, E. (1985). Peridotite composition from the North Atlantic: regional and tectonic variations and implications for partial melting. *Earth and Planetary Science Letters* **73**, 91–104.

Michael, P. J., *et al.* (1994). Mantle control of a dynamically evolving spreading center. *Earth and Planetary Science Letters* **121**, 451–468.

Munker, C., Pfander, J. A., Weyer, S., Buchl, A., Kleine, T. & Mezger, K. (2003). Evolution of planetary cores and the Earth–Moon system from Nb/Ta systematics. *Science*, **301**, 84–87.

Mysen, B. O. & Boettcher, A. L. (1975). Melting of a hydrous mantle: II. Geochemistry of crystals and liquids formed by anatexis of mantle peridotite at high pressures and high temperatures as a function of controlled activities of water, hydrogen, and carbon dioxide. *Journal of Petrology* **16**, 549–593.

Nagasawa, H., Wakita, H., Higuchi, H. & Onuma, N. (1969). Rare earths in peridotite nodules: an explanation of the genetic relationships between basalt and peridotite nodules. *Earth and Planetary Science Letters* **5**, 377–381.

Natland, J. H. (1989). Partial melting of a lithologically heterogeneous mantle: inferences from crystallisation histories of magnesian abyssal tholeiites from the Siqueiros Fracture Zone. In: Saunders, A. D. & Norry, M. J. (eds) *Magmatism in the Ocean Basins. Geological Society, London, Special Publications* **42**,41–70.

Natland, J. H. & Dick, H. J. B. (2001). Formation of the lower ocean crust and the crystallisation of gabbroic cumulates at a very slowly spreading ridge. *Journal of Volcanology and Geothermal Research* **110**, 191–233.

Navon, O. & Stolper, E. (1987). Geochemical consequences of melt percolation: the upper mantle as a chromatographic column. *Journal of Geology* **95**, 285–307.

Nicolas, A. (1989). *Structures of Ophiolite and Dynamics of Oceanic Lithosphere*. Dordrecht: Kluwer Academic, 368 pp.

Nielson, R. L. (1989). Phase equilibria constraints on AFC generated liquid lines of descent: trace element and Sr and Nd isotopes. *Journal of Geophysical Research* **94**, 787–794.

Niu, Y. (1997). Mantle melting and melt extraction processes beneath ocean ridges: evidence from abyssal peridotites. *Journal of Petrology* **38**, 1047–1074.

Niu, Y. (1999). Comments on some misconceptions in igneous/experimental petrology and methodology: a reply. *Journal of Petrology* **40**, 1195–1203.

Niu, Y. (2003). Excess olivine and positive FeO–MgO trend in bulk-rock abyssal peridotites as a consequence of porous melt migration beneath ocean ridges. *EOS Transactions, American Geophysical Union* **84**, Fall Meeting Supplement, Abstract F1540.

Niu, Y. & Batiza, R. (1991). An empirical method for calculating melt compositions produced beneath mid-ocean ridges: application for axis and off-axis (seamounts) melting. *Journal of Geophysical Research* **96**, 21753–21777.

Niu, Y. & Batiza, R. (1993). Chemical variation trends at fast and slow spreading ridges. *Journal of Geophysical Research* **98**, 7887–7902.

Niu, Y. & Batiza, R. (1997). Trace element evidence from seamounts for recycled oceanic crust in the eastern Pacific mantle. *Earth and Planetary Science Letters* **148**, 471–483.

Niu, Y. & Hékinian, R. (1997*a*). Spreading rate dependence of the extent of mantle melting beneath ocean ridges. *Nature* **385**, 326–329.

Niu, Y. & Hékinian, R. (1997*b*). Basaltic liquids and harzburgitic residues in the Garrett transform: a case study at fast-spreading ridges. *Earth and Planetary Science Letters* **146**, 243–258.

Niu, Y. & Lesher, C. M. (1991). Hydrothermal alteration of mafic metavolcanic rocks and genesis of Fe–Zn–Cu sulfide deposits, Stone Hill district, Alabama. *Economic Geology* **86**, 983–1001.

Niu, Y. & O'Hara, M. J. (2003). The origin of ocean island basalts (OIB): a new perspective from petrology, geochemistry and mineral physics considerations. *Journal of Geophysical Research* **108**, 10.1029/2002JB002048, 19 pp.

Niu, Y., Waggoner, D. G., Sinton, J. M. & Mahoney, J. J. (1996). Mantle source heterogeneity and melting processes beneath seafloor spreading centers: the East Pacific Rise, 18°–19°S. *Journal of Geophysical Research* **101**, 27711–27733.

Niu, Y., Langmuir, C. H. & Kinzler, R. J. (1997). The origin of abyssal peridotites: a new perspective. *Earth and Planetary Science Letters* **152**, 251–265.

Niu, Y., Collerson, K. D., Batiza, R., Wendt, J. I. & Regelous, M. (1999). The origin of E-type MORB at ridges far from mantle plumes: the East Pacific Rise at 11°20′N. *Journal of Geophysical Research* **104**, 7067–7087.

Niu, Y., Bideau, D., Hékinian, R. & Batiza, R. (2001). Mantle compositional control on the extent of melting, crust production, gravity anomaly and ridge morphology: a case study at the Mid-Atlantic Ridge 33–35°N. *Earth and Planetary Science Letters* **186**, 383–399.

Niu, Y., Regelous, M. Wendt, J. I., Batiza, R. & O'Hara, M. J. (2002*a*). Geochemistry of near-EPR seamounts: importance of source vs process and the origin of enriched mantle component. *Earth and Planetary Science Letters* **199**, 329–348.

Niu, Y., Gilmore, T., Mackie, S., Greig, A. & Bach, W. (2002*b*). Mineral chemistry, whole-rock compositions and petrogenesis of ODP Leg 176 gabbros: data and discussion. *Proceedings of the Ocean Drilling Program, Scientific Results, 176*. 60 pp. [Online] Available at http://www-odp.tamu.edu/publications/176_SR/chap_08/chap_08.htm. Accessed August 2004.

Niu, Y., O'Hara, M. J. & Pearce, J. A. (2003). Initiation of subduction zones as a consequence of lateral compositional buoyancy contrast within the lithosphere: a petrologic perspective. *Journal of Petrology* **44**, 851–866.

O'Hanley, D. S. (1996). *Serpentinites—Records of Tectonic and Petrological History*. Oxford: Oxford University Press, 277 pp.

O'Hara, M. J. (1977). Geochemical evolution during fractional crystallization of a periodically refilled magma chamber. *Nature* **266**, 503–507.

O'Hara, M. J. (1985). Importance of the 'shape' of the melting regime during partial melting of the mantle. *Nature* **314**, 58–62.

O'Hara, M. J. (1995). Trace element geochemical effects of integrated melt extraction and 'shaped' melting regime. *Journal of Petrology* **36**, 1111–1132.

O'Hara, M. J. (1998). Volcanic plumbing and the space problem—thermal and geochemical consequences of large-scale assimilation in ocean island development. *Journal of Petrology* **39**, 1077–1089.

O'Hara, M. J. & Fry, N. (1996). Chemical effects of small packet crystallization in large magma chambers—further resolution of the highly incompatible element paradox. *Journal of Petrology* **37**, 859–890.

O'Hara, M. J. & Herzberg, C. (2002). Interpretation of trace element and isotope features of basalts: relevance of field relations, petrology, major element data, phase equilibria, and magma chamber modeling in basalt petrogenesis. *Geochimica et Cosmochimica Acta* **66**, 2167–2191.

O'Hara, M. J. & Mathews, R. E. (1981). Geochemical evolution in an advancing, periodically replenished, periodically tapped, continuously fractionating magma chamber. *Journal of the Geological Society, London* **138**, 237–277.

O'Hara, M. J., Fry, N. & Prichard, H. M. (2001*a*). Minor phases as carriers of trace elements in non-modal crystal–liquid separation processes I: basic relationships. *Journal of Petrology* **42**, 1869–1885.

O'Hara, M. J., Fry, N. & Prichard, H. M. (2001*b*). Minor phases as carriers of trace elements in non-modal crystal–liquid separation processes II: Illustrations and bearing on behaviour of REE, U, Th and the PGE in igneous processes. *Journal of Petrology* **42**, 1887–1910.

O'Nions, R. K., Evensen, N. M. & Hamilton, P. J. (1979). Geochemical modeling of mantle differentiation and crustal growth. *Journal of Geophysical Research* **84**, 6091–6101.

Onuma, N., Higuchi, H., Wakita, H. & Nagasawa, H. (1968). Trace element partition between two pyroxenes and host volcanic rocks. *Earth and Planetary Science Letters* **5**, 47–51.

O'Reilly, S. Y. & Griffin, W. L. (1988). Mantle metasomatism beneath western Victoria, Australia: I, Metasomatic processes in Cr-diopside lherzolites. *Geochimica et Cosmochimica Acta* **52**, 433–447.

Peterson, N. L. (1974). Experimental evidence for diffusion mechanisms in pure melts. In: Aaronson, H. I. (ed.) *Diffusion*. Metals Park, OH: American Society of Metals, pp. 47–82.

Phipps Morgan, J. (1987). Melt migration beneath mid-ocean ridge spreading centers. *Geophysical Research Letters* **14**, 1238–1241.

Prinzhofer, A. & Allègre, C. J. (1985). Residual peridotites and the mechanisms of partial melting. *Earth and Planetary Science Letters* **74**, 251–265.

Regelous, M., Niu, Y., Wendt, J. I., Batiza, R., Greig, A. & Collerson, K. D. (1999). An 800 ka record of the geochemistry of magmatism on the East Pacific Rise at 10°30′N: insights into magma chamber processes beneath a fast-spreading ocean ridge. *Earth and Planetary Science Letters* **168**, 45–63.

Rudnick, R. L. & Fountain, D. M. (1995). Nature and composition of the continental crust: a lower crustal perspective. *Review of Geophysics* **33**, 267–309.

Rudnick, R. L., Barth, M., Horn, I. & McDonough, W. F. (2000). Rutile-bearing refractory eclogite: missing link between continents and depleted mantle. *Science* **287**, 278–281.

Salters, V. J. M. & Dick, H. J. B. (2002). Mineralogy of the mid-ocean-ridge basalt source from neodymium isotopic composition of abyssal peridotites. *Nature* **394**, 162–165.

Seyfried, W. S. & Dibble, W. E. (1980). Seawater–peridotite interaction at 300°C, 500 bars: implications for the origin of oceanic serpentinites. *Geochimica et Cosmochimica Acta* **44**, 309–321.

Shen, Y. & Forsyth, D. W. (1995). Geochemical constraints on initial and final depth of melting beneath mid-ocean ridges. *Journal of Geophysical Research* **100**, 2211–2237.

Shimizu, N. (1975). Rare earth elements in garnets and clinopyroxenes from garnet lherzolite nodules in kimberlites. *Earth and Planetary Science Letters* **25**, 26–32.

Sinton, J. M. & Detrick, R. S. (1992). Mid-ocean ridge magma chambers. *Journal of Geophysical Research* **97**, 197–216.

Snow, J., Hart, S. R. & Dick, H. J. B. (1993). 'Orphan' 87 in abyssal peridotites: daddy was a granite. *Science* **262**, 1861–1863.

Snow, J., Hart, S. R. & Dick, H. J. B. (1994). Nd and Sr isotopic evidence for a link between mid-ocean-ridge basalts and abyssal peridotites. *Nature* **371**, 57–60.

Snow, J. E. & Dick, H. J. B. (1995). Pervasive magnesium loss by marine weathering of peridotite. *Geochimica et Cosmochimica Acta* **59**, 4219–4235.

Sparks, D. W. & Parmentier, E. M. (1991). Melt extraction from the mantle beneath spreading centers. *Earth and Planetary Science Letters* **105**, 368–377.

Spiegelman, M. (1993). Physics of melt extraction: theory, implications, and applications. *Philosophical Transactions of the Royal Society of London, Series A* **342**, 23–41.

Spiegelman, M. & Elliot, T. (1993). Geochemical consequences of magma transport for U-series disequilibrium. *Earth and Planetary Science Letters* **118**, 1–20.

Spiegelman, M. & Kenyon, P. (1992). The requirements for the chemical disequilibrium during magma migration. *Earth and Planetary Science Letters* **109**, 611–620.

Spiegelman, M., Aharonov, E. & Kelemen, P. (2001). Causes and consequences of flow organization during melt transport: the reaction infiltration instability in compactable media. *Journal of Geophysical Research* **106**, 2061–2077.

Sun, S.-s. & McDonough, W. F. (1989). Chemical and isotopic systematics in ocean basalt: implications for mantle composition and processes. In: Saunders, A. D. & Norry, M. J. (eds) *Magmatism in the Ocean Basins. Geological Society, London, Special Publications* **42**, 313–345.

Takazawa, E., Frey, F. A., Shimizu, N. & Obata, M. (2000). Whole rock compositional variations in an upper mantle peridotite (Horoman, Hokkaido, Japan): are they consistent with a partial melting process? *Geochimica et Cosmochimica Acta* **64**, 695–716.

Taylor, S. R. & McLennan, S. M. (1985). *The Continental Crust: its Composition and Evolution*. Oxford: Blackwell, 312 pp.

Tiepolo, M., Vannucci, R., Oberti, R., Foley, S., Bottazzi, P. & Zanetti, A. (2000). Nb and Ta incorporation and fractionation in titanian pargasite and kaersutite: crystal–chemical constraints and implications for natural systems. *Earth and Planetary Science Letters* **176**, 185–201.

Toomey, D. R., Wilcock, W. S. D., Solomon, S. C., Hammond, W.C. & Orcutt, J.A. (1998). Mantle seismic structure beneath the MELT region of the East Pacific Rise from P and S tomography. *Science* **280**, 1224–1227.

Turcotte, D. L. & Phipps Morgan, J. (1992). Magma migration and mantle flow beneath a mid-ocean ridge. In: Phipps Morgan, J.,

Blackman, D. K. & Sinton, J. M. (eds) *Mantle Flow and Melt Generation at Mid-ocean Ridges*. *American Geophysical Union Monograph* **71**, 155–182.

Ulmer, P. & Trommsdorff, V. (1995). Serpentine stability to mantle depths and subduction-related magmatism. *Science* **268**, 858–861.

Wade, J. & Wood, B. J. (2001). The Earth's 'missing' niobium may be in the core. *Nature* **409**, 75–78.

Walter, M. W. (1999). Comments on 'Mantle melting and melt extraction processes beneath ocean ridges: evidence from abyssal peridotites' by Yaoling Niu. *Journal of Petrology* **40**, 1187–1193.

Wang, L., Essene, E. J. & Zhang, Y. (1999). Mineral inclusions in pyrope crystals from Garnet Ridge, Arizona, USA: implications for processes in the upper mantle. *Contributions to Mineralogy and Petrology* **135**, 164–178.

Wendt, J. I., Regelous, M., Niu, Y., Hekinian, R. & Collerson, K. D. (1999). Geochemistry of lavas from the Garrett Transform Fault: insights into mantle heterogeneity beneath the eastern Pacific. *Earth and Planetary Science Letters* **173**, 271–284.

Weyer, S., Munker, C., Rekamper, M. & Mezger, K. (2002). Determination of ultra-low Nb, Ta, Zr and Hf concentrations and the chondritic Zr/Hf and Nb/Ta ratio by isotope dilution analyses with multiple collector ICP-MS. *Chemical Geology* **187**, 295–313.

Weyer, S., Munker, C. & Mezger, K. (2003). Nb/Ta, Zr/Hf and REE in the depleted mantle: implications for the differentiation history of the crust–mantle system. *Earth and Planetary Science Letters* **205**, 309–423.

Wetzel, L. R. & Shock, E. L. (2000). Distinguishing ultramafic from basalt-hosted submarine hydrothermal system by comparing calculated vent fluid compositions. *Journal of Geophysical Research* **105**, 8319–8340.

Williams, Q. & Hemley, R. J. (2001). Hydrogen in the deep earth. *Annual Review of Earth and Planetary Sciences* **29**, 365–418.

Wood, B. J., Bryndzia, L. & Johnson, K. E. (1990). Mantle oxidation state and its relationship to tectonic environment and fluid speciation. *Science* **248**, 337–345.

Wood, B. J. & Blundy, J. D. (1997). A predictive model for rare earth element partitioning between clinopyroxene and anhydrous silicate melt. *Contributions to Mineralogy and Petrology* **129**, 166–181.

Yang, H.-J., Sen, G. & Shimizu, N. (1998). Mid-ocean ridge melting: constraints from lithospheric xenoliths at Oahu, Hawaii. *Journal of Petrology* **39**, 277–295.

You, C.-F., Castillo, P. R., Gieskes, J. M., Chan, L. H. & Spivack, A. J. (1996). Trace element behavior in hydrothermal experiments: implications for fluid processes at shallow depths in subduction zones. *Earth and Planetary Science Letters* **140**, 41–52.